



Review

Biochar for Soil Carbon Sequestration: Current Knowledge, Mechanisms, and Future Perspectives

Simeng Li * and Desarae Tasnady

Department of Civil Engineering, California State Polytechnic University, Pomona, CA 91768, USA; datasnady@cpp.edu

* Correspondence: sli@cpp.edu; Tel.: +1-909-869-4787

Abstract: Biochar, a sustainable solid material derived from biomass pyrolysis enriched in carbon, has emerged as a promising solution for soil carbon sequestration. This comprehensive review analyzes the current knowledge on biochar's application in this context. It begins by examining biochar properties and production methods, highlighting its recalcitrant nature as a potential stable carbon sink. The influence of various feedstocks and pyrolysis conditions on various physicochemical properties of biochar and its soil carbon sequestration potential is explored. Mechanisms through which biochar enhances soil carbon sequestration are discussed, including its role as a physical barrier against carbon loss and its ability to promote stable soil aggregates and influence soil microorganisms. Challenges and limitations, such as variations in biochar properties and optimal application rates, are addressed, along with strategies for maximizing biochar effectiveness through amendments. The review concludes by emphasizing the importance of long-term field studies, standardized protocols, and economic assessments to support the widespread adoption of biochar for soil carbon sequestration and its potential in climate change mitigation.

Keywords: biochar; biomass pyrolysis; carbon sequestration; carbon sink; climate change mitigation; mechanisms; physicochemical properties



Citation: Li, S.; Tasnady, D. Biochar for Soil Carbon Sequestration: Current Knowledge, Mechanisms, and Future Perspectives. *C* **2023**, *9*, 67. <https://doi.org/10.3390/c9030067>

Academic Editors: Sergey Mikhalovsky and Rosa Busquets

Received: 20 June 2023

Revised: 5 July 2023

Accepted: 6 July 2023

Published: 7 July 2023



Copyright: © 2023 by the authors. Licensee MDPI, Basel, Switzerland. This article is an open access article distributed under the terms and conditions of the Creative Commons Attribution (CC BY) license (<https://creativecommons.org/licenses/by/4.0/>).

1. Introduction

Climate change poses significant challenges to the global environment, affecting ecosystems [1], weather patterns [2], and human livelihoods [3]. One of the principal contributors to climate change is the excessive release of carbon dioxide (CO₂) and other greenhouse gases (GHGs) into the atmosphere [4]. These emissions are predominantly a result of human activities, such as deforestation and fossil fuel combustion [5–7]. The consequences have been profound, with a remarkable surge in atmospheric CO₂ levels, which have significantly contributed to the escalating global temperature [4,8]. In fact, the average global atmospheric CO₂ concentration in 2020 reached a staggering 412 parts per million (ppm) [9]. If immediate measures to curb emissions are not implemented, it is projected that the atmospheric CO₂ concentration could soar to alarming levels of 600 to 1500 ppm by the year 2030 [10].

Elevated atmospheric CO₂ levels have been associated with substantial soil carbon (C) loss [11,12], posing a potential threat to crop yield and quality [13]. This concern arises at a time when the demand for food is escalating to meet the needs of a rapidly growing global population in the coming decades [14]. Moreover, recent evidence highlights the detrimental health consequences of frequent and prolonged exposure to environments with CO₂ concentrations surpassing 1000 ppm [15]. The impacts encompass a range of consequences, including inflammation, compromised higher-level cognitive functions, a reduction in bone mineral density, the formation of calcium deposits in the kidneys, increased oxidative stress, and impaired endothelial function [15]. In light of these challenges, it becomes imperative to explore and implement strategies that effectively reduce C emissions to reduce gaseous

C in the atmosphere and facilitate long-term soil C sequestration to capture stable C in the soil. Taking decisive measures is imperative to alleviate the detrimental consequences of climate change and secure a sustainable future for both the natural environment and human well-being.

Biochar is a biomass-derived solid material derived mainly through pyrolysis, a thermochemical process completed under high-temperature oxygen-deficit conditions. In recent years, biochar has emerged as a promising soil amendment due to its unique physicochemical properties and interactions with soil systems [16]. When incorporated into soils, biochar enhances soil fertility, nutrient retention, and water-holding capacity. Its porous structure provides a habitat for beneficial microorganisms, improving soil health and promoting plant growth [17]. Furthermore, biochars exhibit a remarkable molecular structure characterized by high chemical and microbial stability. A notable long-term study conducted over eight years investigated the decomposition of biochar derived from ryegrass using compound-specific ^{14}C analysis. The findings revealed an exceptionally slow decomposition rate, with the biochar losing only $7 \times 10^{-4}\%$ of its C content per day under optimal conditions [18]. This implies that it would take nearly 400 years for the biochar to experience a mere 1% reduction in its C content. In a separate study, researchers examined the residence time of biochar derived from *Eucalyptus saligna*, pyrolyzed at $550\text{ }^{\circ}\text{C}$ and subsequently incorporated into soils at $20\text{ }^{\circ}\text{C}$. The study unveiled the significant longevity of this specific biochar, with a mean residence time estimated to range from 732 to 1061 years [19]. These findings provide compelling evidence that reinforces the enduring nature of biochar as an effective C sink, solidifying its potential as a sustainable and long-lasting solution for soil C sequestration.

As biochar continues to gain attention as a potential solution for mitigating climate change and enhancing soil C storage [20,21], there is a pressing need to consolidate the existing knowledge, identify research priorities, and fill the gaps in understanding. This review aims to bridge these knowledge gaps by comprehensively analyzing the properties, mechanisms, challenges, and potential optimization strategies associated with biochar's application for soil C sequestration. Notably, it is worth mentioning that while the application of biochar has the potential to offset atmospheric carbon by promoting biomass yields, the concept of biochar soil carbon sequestration discussed in this paper specifically focuses on increasing the long-term storage of stable organic carbon in the soil. By providing a comprehensive and current overview, this review will contribute to informed decision-making, support the development of standardized protocols, and stimulate further research in this vital area of study. Ultimately, this collective effort will pave the way for the widespread adoption of biochar as an effective and sustainable tool for soil C sequestration in the fight against climate change.

2. Physicochemical Properties of Biochar and Indices for Carbon Sequestration

Biochar's physicochemical properties play a pivotal role as they directly impact its effectiveness and suitability for a wide range of applications [22,23]. High C content, thermal stability, and recalcitrance are essential properties that contribute to biochar's ability to sequester C in the soil over long periods [24,25]. A comprehensive understanding and optimization of these properties can significantly enhance biochar's effectiveness as a reliable and long-term C sink. Various factors, including the feedstock used, pyrolysis conditions, and post-treatment processes, influence the physicochemical properties of biochar [26–28]. In this section, we delve into the properties that are particularly relevant to biochar's potential for C sequestration. Moreover, we explore how these properties are influenced by different factors, shedding light on the intricate relationship between biochar production and its resulting physicochemical characteristics.

2.1. Carbon Content

Biochar is primarily composed of C, accounting for a significant proportion of its composition, typically ranging from around 50% to nearly 90% by weight (Table 1). The high

C content of biochar is essential for its C sequestration potential for several reasons. Firstly, it enables biochar to serve as a stable reservoir for C. When applied to the soil, biochar acts as a sink, effectively capturing and retaining C over extended periods, preventing its release back into the atmosphere as CO₂ [24]. Moreover, the abundant C content of biochar allows for a higher C saturation level in the soil. As biochar is added to the soil, it provides additional C that can exceed the soil's natural C-holding capacity [29]. This surplus C can be effectively sequestered, contributing to an overall increase in soil C stocks and mitigating the net increase in CO₂ in the atmosphere [30]. Furthermore, biochar's high C content, combined with its recalcitrant nature, allows it to persist in the soil for extended periods without significant C loss [31]. This longevity ensures that the sequestered C remains stored in the soil, providing a reliable and long-term solution for C sequestration.

Table 1. Elemental compositions of biochars derived from various types of feedstocks at two different pyrolysis temperatures (400 and 600 °C).

Feedstock	Pyrolysis Temperature	C% (w/w)	O% (w/w)	H% (w/w)	H/C (Atomic)	O/C (Atomic)	Reference
Switchgrass	400 °C	67.26	18.65	3.19	0.57	0.21	[32]
Switchgrass	400 °C	68.24	17.13	2.99	0.53	0.19	[33]
Switchgrass	400 °C	59.60	31.30	4.70	0.95	0.39	[34]
Switchgrass	400 °C	56.69	14.23	3.56	0.75	0.19	[35]
Sludge	400 °C	70.90	16.18	4.49	0.76	0.17	[36]
Sludge	400 °C	48.53	41.34	3.77	0.93	0.64	[37]
Sludge	400 °C	61.47	28.23	2.83	0.55	0.44	[38]
Sludge	400 °C	45.25	49.97	3.74	0.99	0.83	[39]
Oakwood	400 °C	73.45	19.14	3.37	0.55	0.20	[40]
Oakwood	400 °C	74.65	10.41	3.16	0.51	0.11	[33]
Oakwood	400 °C	70.90	12.90	3.60	0.61	0.14	[41]
Oakwood	400 °C	76.41	12.26	2.75	0.43	0.12	[32]
Conocarpus	400 °C	76.83	14.16	2.83	0.44	0.14	[42]
Conocarpus	400 °C	64.17	34.48	0.21	0.40	0.04	[43]
Conocarpus	400 °C	79.31	14.12	2.01	0.30	0.13	[44]
Switchgrass	600 °C	73.47	13.16	2.13	0.35	0.13	[32]
Switchgrass	600 °C	72.72	12.70	2.39	0.39	0.13	[33]
Switchgrass	600 °C	68.15	24.99	2.21	0.39	0.28	[45]
Switchgrass	600 °C	65.31	10.77	2.78	0.51	0.12	[35]
Sludge	600 °C	66.98	26.77	1.24	0.22	0.30	[46]
Sludge	600 °C	82.87	5.35	1.71	0.25	0.05	[47]
Sludge	600 °C	79.76	7.70	1.48	0.22	0.07	[47]
Sludge	600 °C	66.98	26.76	1.24	0.22	0.30	[46]
Oakwood	600 °C	80.44	8.25	2.31	0.38	0.08	[40]
Oakwood	600 °C	78.70	6.76	2.54	0.39	0.06	[33]
Oakwood	600 °C	79.20	13.40	2.00	0.30	0.13	[41]
Oakwood	600 °C	80.72	7.94	1.93	0.29	0.07	[32]
Conocarpus	600 °C	82.93	6.55	1.28	0.19	0.05	[42]
Conocarpus	600 °C	86.71	13.27	0.03	0.12	0.01	[43]
Conocarpus	600 °C	82.35	11.49	0.93	0.14	0.10	[44]

When derived under the same pyrolysis conditions, the C content of biochar is closely related to the feedstock used for its production. A recent meta-analysis reported that wood biochar exhibited a considerably higher average C content of 74.99% compared to corn stover biochar (62.93%) and switchgrass biochar (60.98%) [48]. These differences can be attributed to variations in cellulose, hemicellulose, and lignin contents among the three types of feedstocks [48]. Woody species generally contain 76–109% more lignin and 27–47% more cellulose than herbaceous or grassy species [49–51]. Carbonization is enhanced through the decomposition of lignocellulosic structures and the formation of aromatic structures during pyrolysis [32]. Another study characterized biochars derived from nine different waste types. Across a temperature range of 300 to 600 °C, the biochars derived from poultry litter

(55.06–85.34%), cucumber plant waste (60.95–95.17%), tomato plant waste (62.05–92.74%), and date palm leaf waste (53.72–91.08%) exhibited higher C contents compared to biochars derived from chicken feather waste (51.48–72.02%), cow dung (48.44–79.50%), *Conocarpus* waste (61.87–86.71%), date palm fiber waste (54.21–91.44%), and date palm petiole waste (54.71–84.60%) [43]. In line with findings from previous studies, the biochars with higher C contents were found to originate from waste materials with a higher C content prior to pyrolysis [32,43,48,52].

A consistent trend of increasing C content was observed across various biochars derived from different waste types when subjected to higher pyrolysis temperatures, as reported in numerous previous studies [33,43,51,53,54]. This rise in C content at elevated pyrolysis temperatures can be attributed to the decomposition of organics and the volatilization of elements such as oxygen (O) and hydrogen (H). As pyrolysis temperature increases, the release of organics, tars, and O-/H-containing surface functional groups occurs at a higher rate, while C undergoes intensive thermal decomposition, resulting in aromatization [32]. However, it should be noted that the influence of high pyrolysis temperature on the C content of biochar varies depending on the feedstock type. For instance, wood biochar exhibits a more significant increase in C content than corn stover biochar and switchgrass biochar when exposed to high pyrolysis temperatures (>500 °C) [48], indicating that a higher C content in biochar can be yielded from wood compared to corn stover and switchgrass while considering the same energy expenditure.

2.2. H/C and O/C Atomic Ratios

As the pyrolysis temperature increases, there is a gradual removal of labile non-carbonized organic matter from biochar due to more intensive thermal decomposition [32]. This process leads to the continuous deprivation of vulnerable elements such as O and H through dehydration and decarboxylation [43]. Consequently, biochars with high thermal stability exhibit low atomic ratios of H/C and O/C, indicating a high degree of carbonization and aromaticity [42,44]. The increased aromatic structure of biochar enhances its resistance to chemical reactions and microbial degradations in soils, facilitated by the formation of highly hydrophobic surfaces [55–57]. Therefore, the atomic ratios of H/C and O/C are often used as indicators of biochar's stability [56,58].

The H/C atomic ratio serves as an ideal indicator of biochar's C structure, reflecting the degree of unsaturation and the presence of C-C double bonds [48,59]. A H/C atomic ratio below 0.7 signifies aromatic structures and distinguishes biochar from its raw feedstock, while a ratio below 0.4 indicates high biochar stability and enhanced C sequestration potential with reduced biochar deposition rates [53,56] (Figure 1). In addition, the O/C atomic ratio is employed to classify C combustion residues, with graphite representing the most stable C form. Graphite lacks oxygen, typically having non-detectable or less than 0.5% (*w/w*), indicating nearly oxygen-free C lattice structures [55,60]. In contrast, charcoal and char possess relic structures from untreated biomass, placing them in the category of combustion residues. The threshold O/C ratio for differentiating between these thermal-chemical conversion products and biomass is 0.2, while the dividing line between conversion products and biomass is set at 0.6 [60] (Figure 1). A previous study proposed that biochars with an O/C atomic ratio < 0.2 were anticipated to exhibit a half-life exceeding 1000 years. Biochars with an O/C ratio ranging from 0.2 to 0.6 were found to have intermediate half-lives between 100 and 1000 years. In contrast, biochars with an O/C ratio > 0.6 were likely to degrade by half in less than 100 years [60]. As depicted in Table 1, the H/C atomic ratios of all biochars derived from various feedstocks at 600 °C were consistently below 0.4, with a significant number of these biochars exhibiting an O/C ratio below 0.1. These findings demonstrate that higher pyrolysis temperatures are conducive to the production of biochar with enhanced thermal and chemical stability.

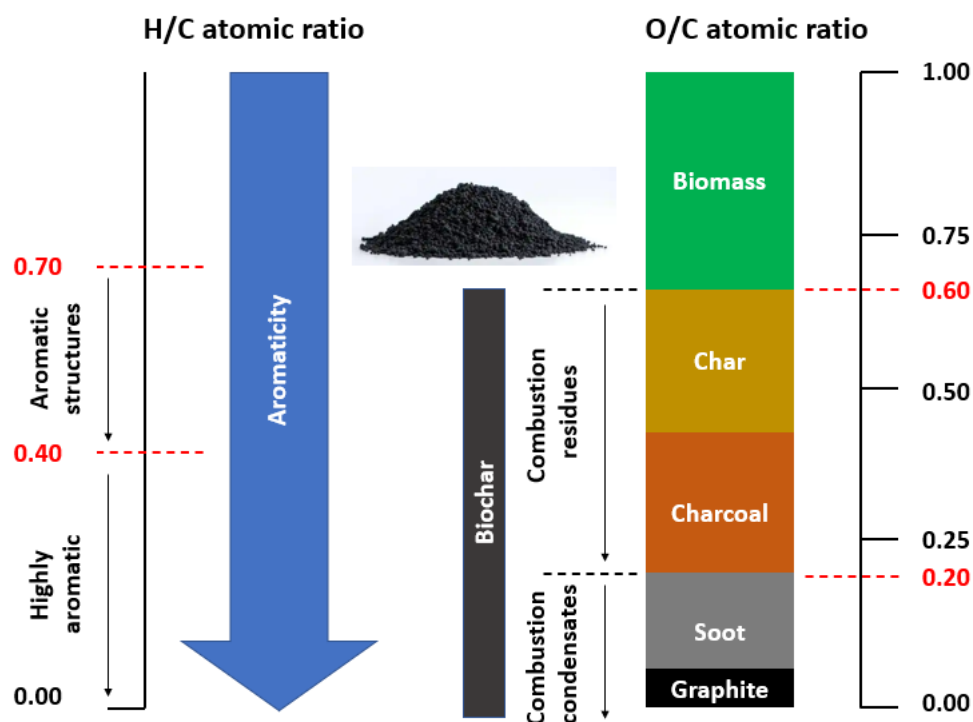


Figure 1. Spectrum and aromaticity of thermochemical biomass conversion products based on H/C and O/C atomic ratios.

By plotting the H/C atomic ratio against the O/C atomic ratio, the van Krevelen diagram can be constructed (Figure 2). Initially designed to visually represent the origin and maturity of petroleum and coal, this diagram has found widespread application in characterizing biochar [56]. It provides valuable insights into the evaluation of biomass components as they undergo thermal decomposition. The variation in H/C and O/C ratios in biochar serves as an indication of the chemical reaction pathways involved in its production [61]. The decrease in H/C and O/C ratios with increasing temperature indicates that the trajectory is linked to dehydration reactions [62]. With the exception of biochars derived from algae and hydrochars with elevated H/C ratios, most biochars exhibit a close correlation between H/C and O/C ratios, often following linear regression patterns [61,63–65].

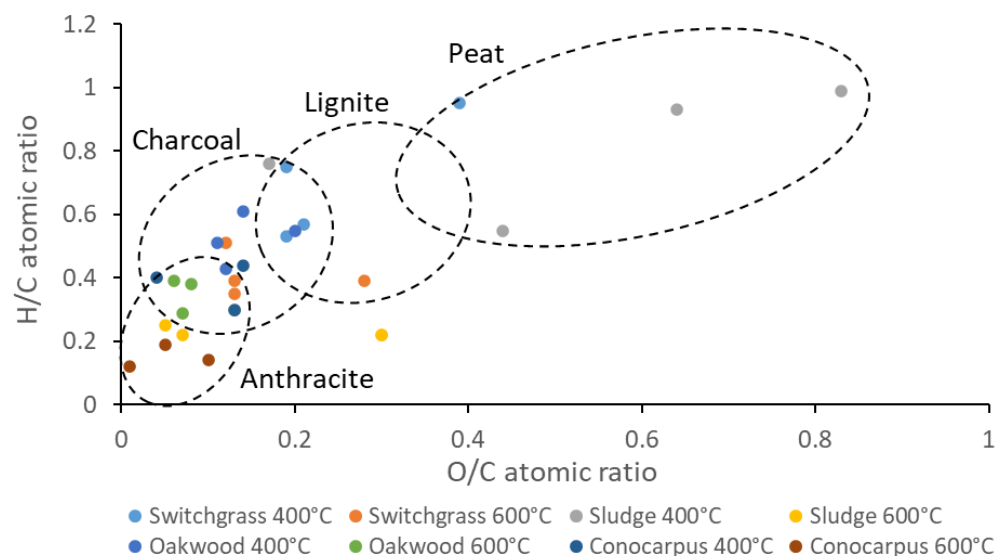


Figure 2. Van Krevelen diagram showcasing the biochars listed in Table 1.

The reduction of O and H levels through thermal treatment is essential to enhance the fuel characteristics of solid fuels, as lower O and H content is desirable [66]. Figure 2 presents a comparison of the atomic ratios of biochars with those of fossil fuels and other materials. The alterations in the H/C and O/C ratios primarily arise from decarbonylation and dehydration reactions, leading to the elimination of volatile oxygenated compounds that contain hydroxyl groups (–OH), such as acetic acid, methanol, and water [66,67]. The findings indicate that the majority of the biochars listed in Table 1 exhibit H/C and O/C ratios that are either superior to or on par with those of fossil fuels, highlighting the potential application of biochar as a sustainable alternative fuel source with improved fuel characteristics [68]. The efficient reduction of volatile oxygenated compounds during biochar production contributes to its energy densification [69], making it a promising option for renewable energy generation and C-neutral fuel technologies.

The utilization of O/C and H/C ratios as indicators of biochar stability was facilitated by the simplicity and cost-effectiveness of ultimate analysis [56]. The impacts of pyrolysis temperature and duration on the aromaticity of biochar were verified through the analysis of solid-state ^{13}C NMR spectra. Figure 3 presents the spectra of biochars derived from different feedstocks and pyrolyzed at various temperatures [70]. It was observed that increasing the pyrolysis temperature beyond 400 °C led to a reduction in aliphatic carbon content and a transformation of carbon compounds into predominantly poly-condensed aromatic structures, as evidenced by a prominent peak at 130 ppm [70]. Furthermore, at a temperature of 600 °C, the lignin signals completely disappeared. The elevation in temperature also induced a significant shift in the aryl region, from 131 to 126 ppm. This shift towards 126 ppm is characteristic of charred residues and indicates the formation of polycyclic aromatic structures with lower hydrogen and oxygen substituents. These modifications signify the conversion of labile compounds into environmentally recalcitrant forms, which are more resistant to degradation.

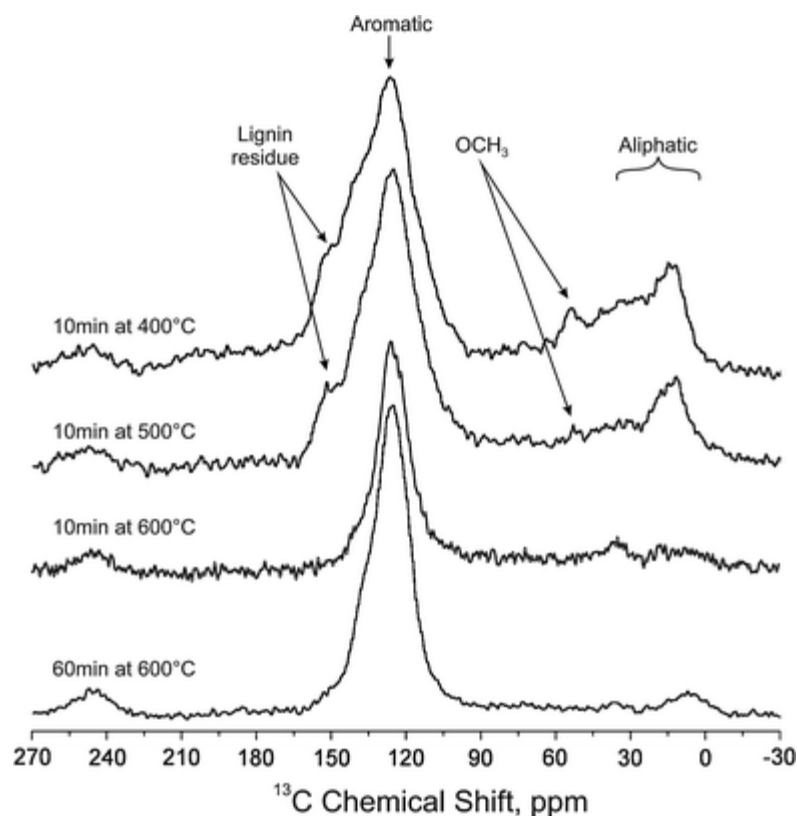


Figure 3. ^{13}C DP/MAS NMR spectra of biochar derived from the pyrolysis of miscanthus at various temperatures and durations. Reproduced from [70] with permission issued by the publisher.

In order to establish a more precise and comprehensive model relationship, it is advisable to conduct longer-term incubation experiments for investigating the dynamics of O/C and H/C. By doing so, a more accurate understanding of biochar stability can be attained, thereby facilitating the wider adoption and application of O/C and H/C analysis in biochar research.

2.3. Fixed Carbon and Volatile Matter

The proximate analysis of biochar is a straightforward way to evaluate the product distribution of biochar under specific heating conditions. The ASTM (American Society for Testing and Materials) defines proximate analysis as the categorization of products into four groups (Figure 4). These groups include: (1) moisture content (MC), (2) volatile matter (VM), comprising the gases and vapors released during pyrolysis, (3) fixed carbon (FC), which represents the non-volatile fraction of biochar, and (4) ash, the inorganic residue remaining after combustion [71]. By measuring the weight difference before and after heating at the specified temperature, the moisture, VM, and ash content of biochar can be directly determined [71]. Utilizing a mass balance approach, the FC can be calculated by subtracting the masses of the other three groups from the sample mass ($M_{biochar}$) using Equation (1) [71]:

$$FC = \frac{M_{biochar} - MC - VM - Ash}{M_{biochar}} \times 100\% \quad (1)$$

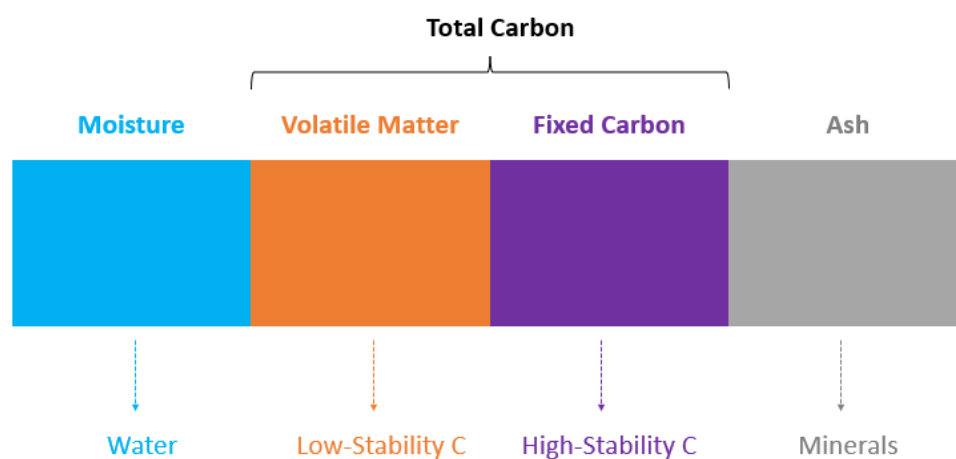


Figure 4. The four groups of products categorized via proximate analysis.

The measurement of FC through proximate analysis differs from the determination of total C through ultimate analysis. Total C includes organic C that escapes as VM during combustion. Thus, FC is closely associated with stable C content, highlighting its relevance as an environmental indicator for biochar's C negativity [72]. A higher FC yield indicates greater potential for biochar as a climate change mitigation tool [43].

In contrast to FC, VM exhibits an inverse trend because increased VM emissions from biochar correspond to a higher relative C content [73]. FC and VM values are utilized to estimate the recalcitrant and labile fractions of biochar, respectively [40,72,73]. Additionally, the ratios of VM/FC and VM/(FC + VM) serve as metrics for assessing biochar stability [73]. Recent cluster analysis suggests that proximate analysis could be an alternative to O/C and H/C ratios in evaluating biochar stability [72]. Specifically, VM/(FC + VM) and H/C were found to be mutually viable alternatives [72]. The cost-effective nature of FC makes it a potential substitute for costly aromaticity measurements or time-consuming stable C assessments, thereby enabling biochar stability determination. Scholars have established a linear relationship ($n = 207$, $R^2 = 0.802$) between O/C and VM/FC, which classifies biochar stability into three categories based on the O/C threshold ($O/C < 0.2$, $0.2 < O/C < 0.6$, $O/C > 0.6$) [73]. Although the relationship between stable C and O/C is relatively weaker, most proxies exhibit correlations with O/C and can be employed for

biochar stability assessment [73]. The associations between these proxies and H/C may be closer to those with O/C, warranting further investigation.

It is worth noting that proximate analysis, conducted at extended durations and specific temperatures (900 °C for VM and 750 °C for ash), may lead to an overestimation of FC [74]. This is attributed to the potential underestimation of ash content due to the volatilization of carbonates and some volatile compounds containing P, K, and S [69]. Other factors such as heating rate and furnace reheating can also pose challenges in terms of reproducibility and consistency [32].

2.4. Thermal Stability Indices

Py-GC-MS (pyrolysis-gas chromatography-mass spectrometry) is an analytical technique that combines the thermal degradation process of pyrolysis with the rapid and real-time analysis provided by GC-MS [75,76]. This powerful method enables the analysis of vapors and gases generated during the pyrolysis of various samples, including biochar [77]. The pyrolysis conditions employed in Py-GC-MS are more severe (e.g., utilizing a pyrolysis temperature of 900 °C) compared to those typically chosen for biochar production. The purpose is to produce distinctive molecular markers from biochar that can be efficiently detected and analyzed by GC-MS [78].

The Thermal Stability Indices (*TSIs*) obtained through Py-GC-MS offer a valuable means of assessing the stability of biochar [77]. To calculate the thermal stability index (*TSI_p*) of individual pyrolysis components, Principal Components Analysis is employed, followed by rescaling the values to a dimensionless proxy ranging from 0 to 100 [79]. Subsequently, the *TSI* of the biochar (*TSI_b*) is determined by multiplying the relative abundance of each pyrolysis component (*i*) with its corresponding *TSI_p*. The resulting values are summed and divided by 100, thus scaling *TSI_b* within the range of 0 to 100, as illustrated by Equation (2).

Biochar's *TSI_b* can be calculated by multiplying the relative abundance of each pyrolysis component (*i*) by its corresponding *TSI* of the pyrolysis component *TSI_p* [79]. The resulting values are summed and divided by 100, ensuring that *TSI_b* is scaled within the range of 0 to 100, as depicted in Equation (2).

$$TSI_b = \sum_i^n [(RP\%)_i \times (TSI)_{pi}] / 100 \quad (2)$$

where, *TSI_{pi}* represents the thermal stability index and $(RP\%)_i$ denotes the relative proportion of a specific pyrolysis component (*b*), and the relative proportion of any individual pyrolysis component (*i*), respectively, *n* is the number of components detected by Py-GC-MS.

The exponential correlation between *TSI_p* and the ratios of benzene to toluene, naphthalene to C₁-naphthalenes, and stable polycyclic aromatic C to total organic carbon (TOC) has been well-established [79]. The recently developed *TSI_p* holds promise as an indicator of biochar stability, potentially influencing its mineralization behavior when implemented in the field [72]. However, the precise value of *TSI_p* for biochar after its incorporation into soil remains uncertain [79]. Additionally, the reliability of Py-GC-MS data may be limited when analyzing highly carbonized biochars, as the peaks in the pyrolysates are barely detectable [56,78]. To gain deeper insights into the highly thermal-stable fractions present in biochars produced at higher temperatures, alternative techniques such as thermally assisted hydrolysis or methylation-GC-MS could be explored [80–82]. These alternative methods offer the potential to obtain more comprehensive information regarding the composition and characteristics of biochars, particularly those produced under extreme thermal conditions.

2.5. Recalcitrance Indices

The assessment of biochar stability can be achieved through thermal stability analysis, which determines the fraction of C capable of withstanding thermal oxidation [32,55,79].

Common techniques such as temperature-programmed oxidation using thermogravimetry (TG) or thermogravimetric analysis (TGA) and differential scanning calorimetry (DSC) are broadly employed to evaluate the oxidative stability of C materials [22,32,83]. During this process, the biochar sample undergoes accelerated decomposition in an oxygen-containing atmosphere, allowing for the measurement of its stability. This method is particularly suitable for biochar stability evaluation, as it minimizes sample alteration at lower temperatures [56].

To quantify the thermal oxidative stability of biochar, the recalcitrance index (R_{50}) has been introduced based on temperature-programmed oxidation [84]. The R_{50} index serves as a comparative indicator of stability in relation to graphite, offering insights into the thermal behavior of biochar. It quantifies the temperature at which 50% of the biochar undergoes oxidation or volatilization ($T_{50,x}$) and relates it to the standardization factor T_{50} , graphite ($T_{50} = 885$ °C) [84]. This calculation, depicted in Equation (3), provides a relative measure of biochar's thermal stability.

$$R_{50} = T_{50,x} / T_{50, \text{ graphite}} \quad (3)$$

The values of $T_{50,x}$ and T_{50} are determined directly from TG thermograms after adjusting for water and ash content using the approach previously described [84]. The R_{50} index for graphite is assigned the highest value ($R_{50} = 1$), while biochars produced under different conditions exhibit R_{50} values ranging from 0.37 to 0.61, with values positively correlated with high-temperature treatment (HTT) [84]. Researchers have utilized the R_{50} index to characterize biochar, observing R_{50} value ranges of 0.45–0.60 [85], 0.33–0.61 [86], and 0.41–0.83 [87]. Remarkably, there is a pronounced inverse exponential correlation between the degradability of biochar (including both abiotic and biotic degradation) over a 1-year incubation period and its resistance to thermal oxidation during thermal degradation [84]. Built upon this relationship, a classification of biochar based on R_{50} values has been proposed: Class A represents the highest stability with $R_{50} \geq 0.70$, Class B indicates lower stability but is still significantly higher than Class C ($R_{50} < 0.50$), which resembles untreated biomass [84].

Further modifications to the R_{50} assessment method have been explored, leading to the introduction of a new index called “gained stability” (GS) to elucidate biochar stability [88]. The GS index is calculated using Equation (4), where $R_{50,x}$, $R_{50,CELL}$, and $R_{50,PCELL}$ represent the R_{50} values of biochar, cellulose, and cellulose char produced at an HTT of 750 °C for 1 h, respectively [89].

$$GS = (R_{50,x} - R_{50,CELL}) / (R_{50,PCELL} - R_{50,CELL}) \quad (4)$$

The “gained stability” index exhibits a strong correlation ($R^2 = 0.97$) with the results obtained from accelerated aging tests conducted using a previously depicted method [89].

During the analysis of R_{50} values for biochars obtained from various feedstocks at different pyrolysis temperatures, Li and Chen (2018) observed significant inconsistencies between the levels of biochar stability indicated by R_{50} values and those suggested by alternative assessment methods, including proximate analysis (VM and FC), elemental analysis (O/C and H/C), and surface functional groups (aromaticity) [32]. For instance, as depicted in Figure 5a, the biosolid feedstock and the biosolid-derived biochar pyrolyzed at 400 °C exhibited the lowest T_{50} values, while the biochar produced at 600 °C displayed the highest T_{50} value. Such T_{50} values, which relate to R_{50} values, demonstrated clear discrepancies with the widely recognized trend of biochar stability, wherein higher pyrolysis temperatures correspond to enhanced stability. Notably, R_{50} values failed to accurately reflect the stability of biochars containing elevated levels of VM and ash, such as those derived from biosolids.

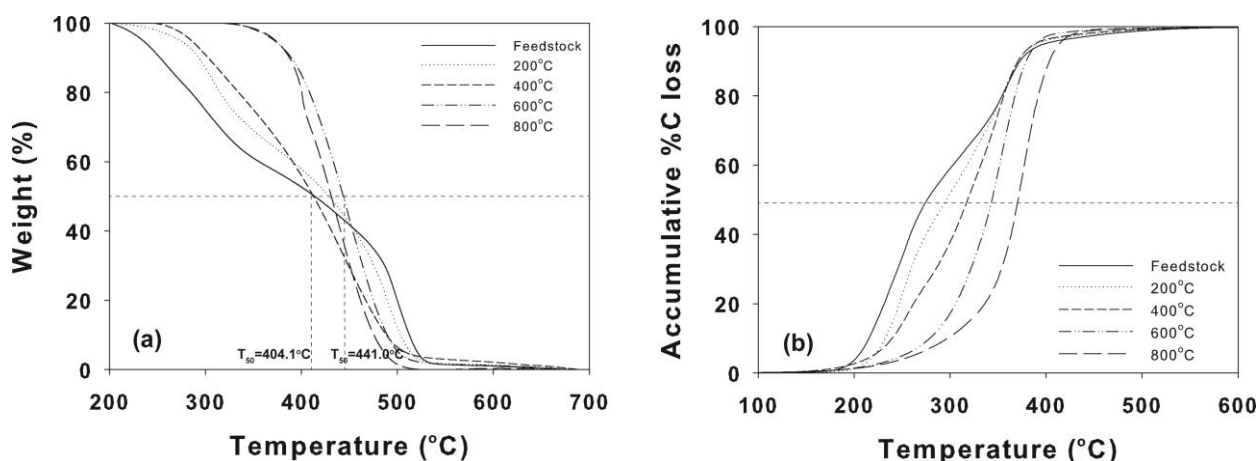


Figure 5. (a) Distributions of T_{50} for biosolid (feedstock) and biochars derived at 200, 400, 600, and 800 °C analyzed based on the thermal gravimetric analysis (TGA) method; (b) distributions of $T_{C,50}$ for biosolid (feedstock) and biochars derived at 200, 400, 600, and 800 °C analyzed based on the multi-element scanning thermal analysis (MESTA) method. Adapted from Li and Chen (2018) [32] with the copyright permission issued by Elsevier.

In their study, Li and Chen (2018) [32] employed multi-element scanning thermal analysis (MESTA) [90] to characterize the cumulative emissions of CO_2 as the temperature ramped from 100 °C to 600 °C, as illustrated in Figure 5b. The cumulative CO_2 emissions were directly linked to C loss resulting from thermal decomposition. By adopting the conceptual framework of R_{50} , Li and Chen proposed a novel recalcitrance index, $R_{C,50}$, which could overcome the limitations associated with TGA-based methods [32]. As shown in Figure 5b, the distribution of $R_{C,50}$ values for the biosolid feedstock and its biochars produced at varying temperatures demonstrated an upward trend of biochar stability with increasing pyrolysis temperature, aligning with the widely accepted conclusion supported by numerous studies [91–94].

2.6. Mean Residence Time

Unlike indirect assessment methods that rely on evaluating aromaticity, degree of aromatic condensation, and oxidation resistance to determine biochar stability, biochar incubation and modeling provide a direct approach to evaluating the stability of biochar [95]. Through this method, the longevity of tested biochar under specific incubation conditions can be determined, often represented as a calculated value such as mean residence time (MRT) based on the modeling of incubation data, specifically the rate of biochar C mineralization [96]. While obtaining the actual biochar stability by incubating biochar until complete degradation and recording the degradation duration would provide the most accurate assessment, the extended time required, often spanning hundreds of years, renders it practically impossible. Existing biochar incubation experiments, excluding charcoal, have only lasted up to a decade [97–99]. Therefore, employing biochar incubation data, including the CO_2 efflux generated from the degradation of biochar during incubation, and utilizing this information to estimate a simulated degradation duration or MRT, offers a pragmatic approach for evaluating the stability of biochar.

The determination of MRT for biochar often entails fitting mineralization data, such as CO_2 efflux, to exponential decay models. This involves calculating the reciprocal of the decay rate [100]. Various models, including one-, double-, and three-pool models, have been developed and employed for data fitting [95,101–103], depending on the assumed number of carbon (C) pools within the biochar [16]. By fitting the mineralization data to exponential decay models, specifically Equations (5) and (6), the MRT can be derived.

$$C_r = \sum_{n=1}^n (C_n \times e^{-k_n \times t}) \quad (5)$$

$$\sum_{n=1}^n C_n = C_0 \quad (6)$$

C_r denotes the remaining biochar C pool at time t , and C_0 represents the initial biochar C pool. Different values of C_n correspond to distinct initial biochar C pools, with n denoting the number of assumed C pools (e.g., $n = 1$ for the one-pool model, $n = 2$ for the double-pool model, and $n = 3$ for the three-pool model). Each decay rate (k_n) associated with the respective C pool can be used to calculate the corresponding *MRT* ($MRT = 1/k_n$), considering that different mineralization rates exist for various biochar C pools. It is worth noting that the one-pool model, which assumes an average decay rate for all C within the biochar, tends to underestimate the *MRT* [95]. Conversely, the double-pool model, which assumes the presence of labile and stable C pools [95], is the most commonly employed approach.

In the realm of biochar incubation and modeling, the evaluation of biochar stability encompasses not only the calculation of *MRT* but also the utilization of half-life time ($t_{1/2}$) and Stable Carbon Protocol (BC_{+100}) as alternative indicators. The half-life time can be derived by multiplying the *MRT* by the natural logarithm of 2, as shown by Equation (7). On the other hand, BC_{+100} refers to the percentage of biochar C predicted to remain stable for over 100 years and can be estimated based on the ratio between hydrogen (H) and oxidizable organic carbon (OOC) following Equation (8). These parameters offer valuable insights into the persistence and degradation behavior of biochar under incubation conditions.

$$t_{1/2} = MRT \times \ln 2 \quad (7)$$

$$BC_{+100} = 1.05 - 0.616 \times \left(\frac{H}{OOC} \right) \quad (8)$$

The utilization of BC_{+100} as a parameter offers a valuable approach to establishing relationships between biochar properties and stability. This framework enables the convenient use of biochar properties, such as proximate analysis results, as proxies to assess biochar stability. For instance, the threshold lines of $H/OOC < 0.4$ and $0.4 < H/OOC < 0.7$ indicate that 70% (BC_{+100} value, “highly stable”) and 50% (BC_{+100} value, “stable”) of biochar C would remain stable in the soil after 100 years, respectively [104].

2.7. Other Physicochemical Properties and Parameters Relevant to Carbon Sequestration

Several other physicochemical properties and parameters of biochar, encompassing particle size, surface area, porosity, pore size distribution, pH, and cation exchange capacity (CEC), play a crucial role and indirectly affect its potential for C sequestration.

2.7.1. Particle Size and Surface Area

The C sequestration potential of biochar is significantly influenced by its particle size and surface area. Smaller particle sizes (diameter of less than 0.045 mm) and larger surface areas (exceeding 100 m²/g) offer numerous advantages. Initially, reducing the particle size enhances the contact area between the biochar and its surrounding environment, facilitating the interaction and adsorption of GHGs such as CO₂, CH₄, and N₂O [17]. This improved contact allows for more efficient capture and retention of C within the biochar structure. Recent research conducted on biochar derived from various-sized *Camellia oleifera* fruit shells demonstrated that the smallest shell sizes (ranging from 0.5 to 2 mm) were associated with the lowest CO₂ and N₂O emission rates [105]. Larger particles (2–5 mm or 5–10 mm) generally have a lower surface area-to-volume ratio, which can limit microbial accessibility and subsequent degradation. Therefore, larger biochar particles may exhibit reduced CO₂ efflux due to decreased microbial activity and slower decomposition rates.

Moreover, biochars with increased surface areas have greater numbers of binding sites for organic C molecules, thereby enhancing their C sequestration capacity [106]. This augmented surface area enables a higher degree of organic matter adsorption, effectively transforming the biochar into a C reservoir within the soil [107]. Additionally, the surface area of the biochar exerts an influence on microbial activity and nutrient cycling in the soil. Soil microorganisms can attach themselves to the biochar surface, leading to enhanced microbial colonization and activity [108]. This microbial activity contributes to the decomposition of organics and the formation of stable C compounds, thereby promoting long-term C sequestration [109].

However, it is important to consider the interaction between biochar and soil microbial activities in relation to soil characteristics. An intriguing finding from a recent meta-analysis indicates that the incorporation of biochar into sandy soils exerts a substantial impact on the mineralization of soil organic matter (SOM), resulting in a remarkable stimulation of approximately 20.8% [96]. It is interesting to note that biochar application can lead to increases in indigenous SOM in many soil types [110]. Biochar can act as a substrate and provide a habitat for microorganisms, enhancing their activity and promoting the decomposition of organic matter [111]. This can result in the stimulation of microbial communities and an increase in SOM turnover rates, leading to greater soil carbon mineralization [111]. However, in sandy soils, which typically have lower organic matter content and limited water and nutrient-holding capacity, the introduction of biochar may alter the microbial dynamics in ways that could promote the biological oxidation of SOM [112]. The increased availability of labile carbon from biochar can potentially fuel microbial activity, leading to accelerated decomposition of both biochar and indigenous organic matter [112]. These findings emphasize the importance of considering soil type and its specific characteristics when assessing the impact of biochar on indigenous SOM. It also highlights the need for site-specific studies to understand the interactions between biochar, soil properties, and microbial processes in different soil types. To fully comprehend the intricate dynamics at play, additional exploration is warranted into the interplay between abiotic and biotic processes, as well as the specific properties of both biochar and soils, which collectively shape the decomposition of biochar.

2.7.2. Porosity and Pore Size Distribution

Porosity in biochar refers to the extent of empty spaces or pores within its structure, whereas pore size distribution pertains to the range of pore sizes present. These characteristics hold significant implications for C sequestration.

The presence of high porosity in biochar offers several advantages for C sequestration. Firstly, it amplifies the available surface area for interactions with C-containing compounds, facilitating the adsorption and retention of C [113]. This ability transforms biochar into a reservoir for organic C within the soil. Secondly, the porous nature of biochar creates habitats and colonization sites for beneficial microorganisms [114].

Pore size distribution within biochar further contributes to its C sequestration potential. Distinct pore sizes accommodate the adsorption of different compounds and molecules [115]. Micropores, characterized by diameters below 2 nm, exhibit exceptional proficiency in adsorbing GHGs like CO₂, CH₄, and N₂O [115]. Mesopores, ranging from 2 to 50 nm, facilitate the adsorption of water, organic matter, and nutrients [116]. The ability to hold water and preserve dissolved organic C enhances the stability and persistence of C within the soil [117]. Furthermore, mesopores create favorable conditions for the colonization of beneficial microorganisms, thereby promoting their activity and enriching soil C cycling processes [108]. Macropores, exceeding 50 nm in diameter, enable the movement of air, water, and nutrients throughout the soil profile. Improved soil aeration and water infiltration consequentially benefit plant growth and microbial activity, indirectly influencing C sequestration processes [118].

The combination of these varied pore sizes within biochar optimizes the efficient capture, retention, and cycling of C within the soil ecosystem. It facilitates the adsorption

of GHGs, provides a conducive habitat for beneficial microorganisms, and contributes to the long-term stability of C compounds.

2.7.3. Biochar pH and Cation Exchange Capacity (CEC)

The pH and cation exchange capacity (CEC) of biochar have a profound influence on its interactions with the soil environment, organics, and plants. The soil pH is an important factor affecting C dynamics in the soil, while CEC refers to the ability to attract, retain, and exchange cations (positively charged ions) with the surrounding soil environment. Biochar typically exhibits high pH values, commonly exceeding 8.0, indicating its alkaline nature [43,119]. Meanwhile, the incorporation of biochar into soils has been shown to substantially increase the CEC of the amended soils [114,120]. These elevated alkalinity and CEC levels in soils exert noteworthy impacts on soil properties and processes associated with C sequestration.

One of the key mechanisms by which biochar pH influences C sequestration is through its impact on soil microbial activity [121]. Soil microorganisms play a crucial role in the decomposition of organics and the cycling of C in the ecosystem [108]. The pH of biochar can influence the composition and activity of microbial communities in the soil [108]. Alkaline biochar can create an environment that favors certain microbial populations, leading to changes in the decomposition rates of organics and the stabilization of C compounds [108]. This can result in enhanced C sequestration over time. As an example, a recent field study demonstrated a reduction or similarity in soil microbial activity and abundance across the majority of biochar-amended field sites. This was evident through a decrease in dehydrogenase activity and a lower rate of C mineralization [111].

Furthermore, the pH of biochar can influence nutrient availability and uptake by plants [122,123]. Alkaline biochar can increase the pH of acidic soils, making them more favorable for plant growth [122,123]. This can lead to increased biomass production, which in turn contributes to higher C sequestration through enhanced plant C inputs into the soil [124].

It is worth noting that the specific effects of biochar pH on C sequestration can vary depending on the characteristics of the soil and the biochar itself [109]. Different soil types and biochar feedstocks can exhibit varying responses to changes in pH [108,114]. Therefore, it is essential to consider the interactions between biochar pH, soil properties, and specific environmental conditions in order to fully understand and harness the potential of biochar for C sequestration.

3. Mechanisms of Biochar for Carbon Sequestration

Biochar's effects on C sequestration are multifaceted and involve several interconnected mechanisms, as shown in Figure 6. Each mechanism contributes to the overall process of soil C sequestration, and their combined effects result in enhanced C storage in the soil.

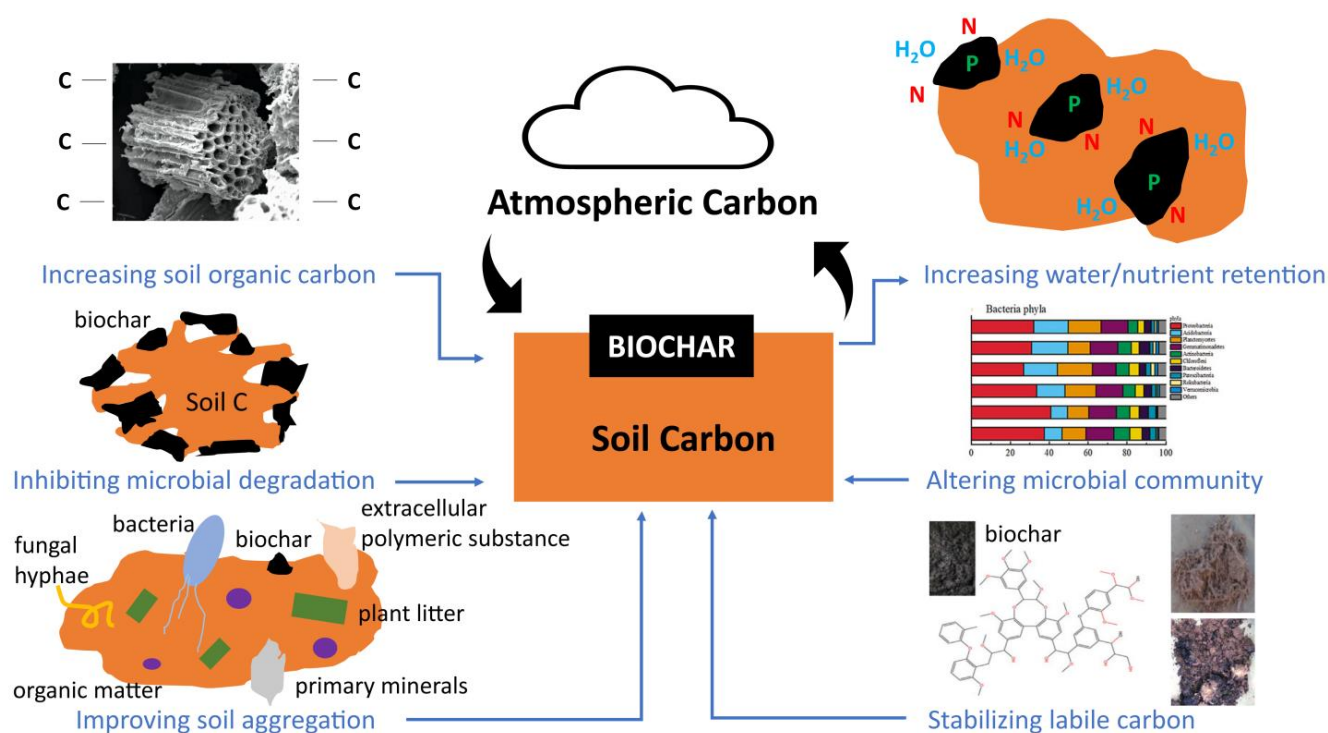


Figure 6. Major effects of biochar on enhancing soil carbon sequestration.

3.1. Increased Soil Organic Carbon (SOC) Input

When biochar is added to the soil, it acts as a stable form of C, providing a long-term source of organic C [96]. Biochar's resistance to decomposition allows it to persist in the soil for extended periods, effectively increasing the overall input of SOC [55]. By conducting an extensive four-year field study in north China, along with controlled laboratory incubation experiments manipulating moisture and temperature, scientists have uncovered significant insights into the influence of biochar incorporation on SOC sequestration. The combination of long-term field observations and controlled conditions in the laboratory has provided valuable findings concerning the effects of biochar addition on the storage of SOC [125]. The results demonstrated that the incorporation of biochar resulted in a substantial increase in average annual SOC sequestration rates, ranging from 31.8% to 47.8% (equivalent to 369.8–556.6 kg ha⁻¹ yr⁻¹), ultimately leading to a higher C stock compared to the control group.

However, it is important to note that the study also revealed an increase in the temporal variability of SOC due to biochar addition. This variability stemmed from the heightened sensitivity of SOC mineralization to temperature fluctuations in the 0–10 cm layer and moisture variations in the 10–20 cm layer, thus imposing limitations on the full potential of SOC sequestration. To ensure an optimal and cost-effective approach, the study suggests that biochar addition should be carefully controlled within a specific rate range of 1.8 to 3.6 t ha⁻¹ yr⁻¹ for the studied region in the North China Plain. This range allows for the balanced consideration of SOC sequestration benefits while mitigating potential drawbacks associated with increased temporal variability. These findings shed light on the effectiveness of biochar as a soil amendment for enhancing SOC sequestration, while emphasizing the need for region-specific management strategies to achieve optimal outcomes in terms of C sequestration and overall soil health.

3.2. Protection against Microbial Decomposition

Biochar plays a crucial role in physically safeguarding labile organic C, including rhizodeposits and microbial necromass, against microbial decomposition [30]. Its recalcitrant structure and remarkable stability form a protective barrier that shields the embedded

organic C from microbial activity [126]. This protective function significantly reduces the rate of C mineralization, thus accumulating SOC as a result [111]. In a recent study conducted in a bamboo plantation, the application of biochar demonstrated notable effects compared to the control group. It led to a significant increase in aromatic C content and RubisCO enzyme activity, while simultaneously reducing β -glucosidase and cellobiohydrolase (CBH) activities [127]. Moreover, there was a positive correlation ($p < 0.01$) between soil heterotrophic respiration and β -glucosidase and CBH activities, whereas a negative correlation ($p < 0.05$) was observed with RubisCO enzyme activity. Structural equation modeling further revealed that biochar influenced heterotrophic respiration by increasing the proportion of the recalcitrant soil C fraction and decreasing β -glucosidase and CBH activities that were associated with carbohydrate and cellulose decomposition in the soil [127].

Furthermore, a recently published field study demonstrated that the mineralization of native SOC in the soil was mitigated by 18% after two rounds of biochar applications spanning a decade [30]. This effect was attributed to the reduced specific enzyme activities resulting from the protective shielding provided by biochar [111]. On a global scale, it has been estimated that the preservation and restoration of soil C could sequester approximately 5.5 Pg of CO₂ annually, representing 25% of the potential of natural climate solutions for C dioxide removal through conservation, restoration, and improved land management practices [128].

These findings underscore the significant role of biochar in physically protecting labile organic C from microbial decomposition, leading to enhanced SOC accumulation. The use of biochar as a soil amendment holds immense potential for climate change mitigation and the adoption of sustainable land management practices on a global scale.

3.3. Enhanced Soil Aggregation

Biochar exhibits the remarkable ability to enhance soil aggregation, the process of forming cohesive soil aggregates or clumps [129]. The porous nature of biochar provides favorable habitats for beneficial soil microorganisms, fostering their activity and contribution to the formation of stable soil aggregates [130]. These aggregates serve as a protective environment for SOC, effectively impeding its decomposition and facilitating its long-term sequestration [31].

In order to explore the impact of pre-existing soil organic matter on the stability of biochar in comparison to labile organic additions, a comprehensive study was conducted [131]. The findings revealed that the application of biochar resulted in a significant 27% reduction in the rate of CO₂-C loss [131]. Intriguingly, a considerably higher proportion of carbon (6.8 times) was discovered in the intra-aggregate fraction per unit of respired carbon, indicating a more efficient mechanism of stabilization in addition to the inherent chemical recalcitrance of biochar [131]. Fourier-transform infrared (FTIR) spectroscopy analysis unveiled that in soils with limited soil organic carbon (SOC) content, the application of biochar led to the enrichment of aromatic-C, carboxyl-C, and traces of ketones and esters. These transformations were primarily observed within unprotected organic matter and aggregates [131]. These results provide compelling evidence that biochar not only exhibits superior stability but also outperforms labile organic matter additions, such as green manure, in terms of effective carbon stabilization [131].

Another study employed quantitative evaluations to assess the impact of biochar on aggregate stability in simplified soil systems [132]. Over a two-year field study, it was observed that soil aggregate stability increased with the rate of biochar application [132]. Theoretical calculations indicated that both electrostatic repulsion and van der Waals attraction forces increased upon biochar incorporation, while the net pressure of soil internal forces decreased [129]. The observed soil aggregate stability aligned well with the predictions of the theoretical calculations [129]. The introduction of biochar reduced the net pressure of soil internal forces, thereby stabilizing the soil aggregates [31,133]. This study, utilizing a mono-cationic model system, provides valuable insights into the

intricate mechanisms underlying the interaction between biochar and minerals within soil systems [129].

It is important to note that the interactions between added biochar and different soil types and structures may yield contrasting effects and warrant further investigation. Diverse outcomes were observed when varying quantities of biochar were applied to different soil types, yielding distinct effects on wet aggregate stability [134]. In sandy loam soils, the addition of biochar increased the soil surface area, compensating for the initially low SOC content and thereby facilitating SOC-controlled aggregation [134]. Conversely, in clay soil, a higher dosage of biochar (40 t ha^{-1}) amplified repulsive forces among particles carrying the same charge and monovalent cations. This led to chemical disturbances and some breakdown of aggregates, which was not observed with the lower dosage of biochar (20 t ha^{-1}) [134]. Moreover, the pore structure within clay aggregates was altered, exhibiting a shift towards an increased presence of micropores ($30\text{--}5 \mu\text{m}$, increased by 29% compared to the control) and ultramicropores ($5\text{--}0.1 \mu\text{m}$, increased by 22% compared to the control) upon biochar addition, which contributed to aggregate stabilization [134]. Collectively, these results emphasize the positive influence of biochar on aggregate stability, thereby enhancing the physical fertility of soils, particularly those characterized by a coarse texture and low organic C content.

3.4. Increased Water and Nutrient Retention

Biochar has a high CEC and moderate alkalinity, allowing it to attract and retain water and nutrients (particularly N and K) in the soil [17,33]. By retaining water and nutrients such as nitrogen and phosphorus, biochar facilitates improved nutrient availability for plants, thus reducing the risk of nutrient loss from the soil system [123,124]. This also leads to increased plant growth and productivity, which in turn promotes the input of organic C into the soil through root exudates, rhizodeposition, and plant residues [122,135]. The additional C inputs into the soil contribute to the accumulation of SOC over time.

The increased water retention capacity of biochar creates favorable conditions for the decomposition of organic matter [109]. By maintaining higher soil moisture levels, biochar can promote the activity of soil microorganisms involved in organic matter decomposition and nutrient cycling [108]. Over the course of a ten-year field experiment, it was observed that the application of biochar resulted in significant improvements in soil C content. The addition of biochar led to an increase in the soil's inorganic C content ranging from 3.2% to 24.3%. Furthermore, there was a substantial enhancement in the soil organic carbon (SOC) content, ranging from 15.8% to 82.2% [136]. These findings highlight the effectiveness of biochar in promoting C sequestration in the soil, underscoring its potential as a valuable strategy for mitigating C dioxide emissions and enhancing soil fertility.

3.5. Altered Soil Microbial Community

The impact of biochar on the soil microbial community is a critical determinant in soil C sequestration processes. Biochar possesses the capacity to shape and modify the composition and activity of soil microbial populations, thereby exerting a profound influence on C dynamics within the soil matrix.

Primarily, biochar functions as a habitat and substrate for beneficial microorganisms, capitalizing on its porous structure to foster microbial colonization and stimulate their growth and metabolic activity [137]. These microorganisms, encompassing bacteria and fungi, engage in intricate interactions with organic matter, orchestrating its decomposition and the subsequent transformation of C compounds within the soil [108]. A comprehensive four-year field investigation revealed that biochar application engendered notable increments in SOC content and the recalcitrant organic C fraction, ranging from 11.02% to 22.13% and 18.41% to 32.31%, respectively, at biochar application rates of 6 and 12 t ha^{-1} [138]. Remarkably, the augmented proportion of the recalcitrant organic C fraction surpassed that of SOC [138]. Simultaneously, biochar application induced a reduction in bacterial abundance by 9.25% to 35.77% while exerting an impact on bacterial community structure by

enhancing the relative abundance of *Chloroflexi phylum*, known for its low C mineralization rate and potent C fixation capabilities. Dissolved organic C emerged as a pivotal factor influencing bacterial abundance and community structure [138]. In contrast, the addition of 12 t ha⁻¹ of biochar resulted in a reduction of fungal diversity by 12.45%, accompanied by notable changes in the composition of the fungal community. Specifically, the relative abundances of the *Sordariomycetes* and *Tremellomycetes* classes were amplified, favoring the formation of SOC. This alteration in fungal community structure highlights the potential role of these specific fungal groups in facilitating SOC accumulation through their interactions with biochar [138]. By promoting the growth of these beneficial microorganisms, biochar indirectly facilitated the formation of stable C compounds, thereby augmenting the process of C sequestration.

Biochar amendments possess the capacity to modify enzymatic activity through their influence on microbial community composition and metabolic processes, thereby instigating alterations in the rates of organic matter decomposition and subsequent C sequestration. A recent study demonstrated that the application of biochar, derived from invasive weeds and prepared at 450 °C, at reclaimed coal mine sites resulted in a significant increase in the geometric mean of enzymatic activity index by 37.9% and 75.8% at biochar application rates of 10 and 20 t ha⁻¹, respectively, signifying improved microbial activities [139]. Moreover, at an application rate of 20 t ha⁻¹, the soil exhibited significantly higher recalcitrant C content, indicative of a greater potential for C sequestration through biochar application. Additionally, total C stock demonstrated increments of 13% and 91% at biochar application rates of 10 and 20 t ha⁻¹, respectively, with CO₂ sequestration increasing by 13% and 91% at the corresponding biochar application rates [139].

3.6. Stabilization of Labile Carbon

The non-stable fraction of biochar holds significant importance alongside its stable counterpart, and there are two key reasons for this. Firstly, the labile fraction that emerges from biochar during its storage in the soil is highly likely to influence microbial activity, thereby impacting the overall functioning of the soil system, including the equilibrium of indigenous labile carbon pools [112]. This highlights the dynamic nature of biochar's labile fraction and its potential to influence soil processes. Secondly, the non-stable fraction, particularly its less labile component, has the potential for further stabilization, thereby contributing to an increased yield of the stable biochar fraction [92]. This implies that even the non-stable fraction of biochar can play a role in long-term carbon sequestration by transitioning into a more stable form over time.

Biochar plays a crucial role in stabilizing labile or easily decomposable C compounds in the soil, thereby facilitating long-term C sequestration [131,140]. While carbon mineralization rates were frequently observed to be higher in soil amended with biochar, it is important to note that this increase was primarily attributed to the rapid utilization of a relatively small labile fraction within the biochar itself [141]. It is crucial to emphasize that biochar did not induce priming effects leading to the accelerated decomposition or loss of native soil organic matter. On the contrary, there were instances where negative priming occurred, resulting in lower rates of carbon mineralization in biochar-amended soil [19,103]. This phenomenon can be attributed to the stabilization of labile soil carbon through the presence of biochar.

Biochar accomplishes the stabilization of labile carbon through several key mechanisms. Firstly, biochar possesses a recalcitrant and stable structure that acts as a physical barrier, safeguarding labile C from microbial decomposition [142]. The porous nature of biochar provides a protective environment, slowing down the rate of C mineralization and prolonging the residence time of labile C in the soil [111]. Secondly, biochar exhibits a high surface area and has the ability to adsorb organic compounds [109]. Labile C molecules can attach to the surface of biochar particles, forming stable associations that reduce their susceptibility to microbial degradation [140]. This sorption mechanism effectively retains labile C in the soil, impeding its rapid decomposition. Furthermore, as mentioned earlier,

biochar's impact on chemical interactions, aggregate formation, and alterations in the microbial community also contribute to the stabilization of labile C in the soil [108,117,134]. These processes lead to the formation of more stable C compounds, augmenting the sequestration of labile C.

Overall, biochar's ability to physically protect labile C, its adsorption capacity, and its influence on chemical interactions, aggregate formation, and microbial communities collectively contribute to the stabilization of labile C in the soil, fostering long-term C sequestration. It is worth noting that the specific mechanisms and their relative importance in soil C sequestration can vary depending on factors such as biochar properties, soil type, climate conditions, and land management practices.

4. Current Challenges and Limitations

4.1. Feedstock Availability and Sustainability

The production of biochar necessitates a consistent supply of biomass feedstock. However, guaranteeing a sustainable and adequate feedstock supply can prove challenging, particularly when considering large-scale biochar applications. Emphasizing environmentally friendly feedstock sources that do not compete with food production or harm ecosystems is of utmost importance. Recent research delved into the viability of various feedstocks for biochar production, including grape residues, distillers grains, sugarcane residues, palm oil residues, apple pomace, and sawdust [143]. Notably, agricultural residues yielded higher biochar yields than forestry residues. Out of all the agricultural residues examined, grape residues displayed the most favorable biochar yields, showcasing their potential as a viable biomass source for biochar production. Conversely, apple pomace and palm oil fiber yielded the lowest quantities of biochar, indicating their limited suitability for large-scale biochar production [143]. The study further revealed that to achieve a self-sustaining process that generates biochars with optimal physicochemical properties and reasonable yields, biochar production is best performed at temperatures ranging from 450 to 550 °C and vapor residence times ranging from 2 to 5 s, achieved by burning the product gases and part of the bio-oil vapors [143].

From an economic standpoint, biochar production demonstrates sustainable strength considering the abundance in both forest and agricultural residues [43,86,127], enabling the utilization of biochars derived from wood residues with their potential for higher heating value and application in metallurgical and power generation contexts [45,50], along with the reduction of on-site CO₂ emissions [23,105]. Similarly, biochars derived from agricultural residues possess selective physicochemical characteristics and higher plant nutrients, facilitating improved nutrient recovery, nutrient use efficiency, and environmental applications [24,69]. Furthermore, establishing a sustainable biomass supply chain from the biomass supply location to the biomass conversion site necessitates thorough analysis and strategic assurance.

Typically, the effectiveness and applicability of biochar can be influenced by a range of inorganic and organic pollutants, encompassing heavy metals, polycyclic aromatic hydrocarbons (PAHs), polychlorinated biphenols (PCBs), dioxins, and furans [38,46,144]. As a result, when utilizing biochar, concerns arise regarding the environmental impact associated with emissions (during ironmaking and energy generation), the mobility and bioavailability of potentially toxic elements (PTEs), and the leaching of these elements during activities such as soil improvement and pollutant reduction [145]. In the case of biochar produced at higher temperatures, the concerns related to toxicity are comparatively diminished. This is attributed to the decreased volatility of PTEs within biochar and their concentration in the residual ash, which differs from the elevated emissions often associated with coal or coke conversion processes utilized in ironmaking [144,146]. Additionally, the leaching and bioavailability of toxic trace elements in biochar are less likely, especially in cases of higher pH [39], which are generally alkaline for most biochar instances, rendering trace elements immobile. However, the mobility of oxyanions cannot be entirely discounted [147].

At elevated pyrolysis temperatures ($>650\text{ }^{\circ}\text{C}$), the formation of PAHs is attributed to two primary mechanisms: Diels–Alder-type reactions and the deoxygenation of oxygenated aromatic compounds [148]. It is highly influenced by factors such as pyrolysis temperature, gas phase residence time, and the composition of the material being pyrolyzed [149]. Studies have shown that PAH yields from the secondary gas-phase pyrolysis of various biomass-derived tars, including cellulose, glucose, pectin, and chlorogenic acid, increase as the pyrolysis temperature and gas-phase residence time increase [150,151]. Conversely, at lower pyrolysis temperatures ($400\text{--}600\text{ }^{\circ}\text{C}$), PAH formation is believed to occur through a carbonization process [152]. In this process, the solid char residue undergoes chemical transformations and rearrangements, leading to the formation of more condensed polycyclic aromatic structures. This transformation involves a series of reactions, including dehydration, decarbonylation, decarboxylation, dehydrogenation, and cross-linking [152]. As the temperature of the char increases from 300 to $650\text{ }^{\circ}\text{C}$, polycyclic aromatic compounds are generated and subsequently released from the solid char residue into the gas phase. The evolution profiles of PAHs from the solid residue suggest that smaller PAHs with 2–3 rings are released from the char first, reaching their maximum concentration at a slightly lower temperature compared to larger PAHs with 4–5 rings [152]. In addition to PAH formation, the concentration of PAHs in biochar is also influenced by vaporization. Interestingly, both of these mechanisms, PAH formation and vaporization, are enhanced with increasing pyrolysis temperature [153]. As the pyrolysis temperature rises, the formation of PAHs generally increases due to the more favorable conditions for their generation. However, at the same time, the elevated temperature can lead to increased vaporization of PAHs from the biochar [153]. This interplay between the two mechanisms may explain the lack of a consistent trend in PAH content in biochar with temperature reported in the literature. Nonetheless, further research is needed on this front, as comprehensive systematic studies, particularly regarding the occurrence modes, total concentrations, behavior, and fate of hazardous contaminants in biochar, along with their chemical speciation or sequential extraction, are scarce.

To mitigate the environmental and health impacts associated with the release of harmful gases during the pyrolysis processes for biochar production, it is crucial to adopt appropriate pyrolysis techniques and technologies. One such example is the use of retort kilns, which have been reported to significantly reduce the emissions of products of incomplete combustion. Retort kilns operate by recirculating and combusting the pyrolysis gases internally, thereby lowering harmful emissions. Additionally, the heat generated in this process can sustain the pyrolysis process without relying on heat from the feedstock itself [154]. Furthermore, the implementation of advanced emission control systems, such as scrubbers and filters, can play a vital role in capturing and treating harmful gases before their release into the atmosphere [155]. These systems effectively remove pollutants and particulate matter, contributing to improved air quality and minimizing the environmental impact of biochar production.

To ensure the long-term sustainability of biochar production, ongoing research and the implementation of strategies to minimize the release of harmful gases are crucial. It is imperative to explore and develop more sustainable biochar production methods that prioritize both environmental and human well-being. This can involve continuous advancements in pyrolysis technologies [52,66], the use of renewable energy sources for heat generation [156,157], and the development of comprehensive emission control measures [158]. By adopting these strategies and investing in research and development, the biochar industry can significantly reduce its environmental footprint and contribute to a more sustainable and responsible approach to carbon sequestration. The ongoing commitment to minimizing harmful emissions from biochar production will support the broader goal of mitigating climate change and safeguarding human health.

4.2. Production Costs, Prices, and Scalability

Biochar production encompasses various processes, including feedstock collection, pyrolysis, and conditioning. These processes can be resource-intensive and costly, impacting the economic viability of large-scale biochar production and application. Therefore, it is crucial to explore cost-effective and scalable production methods to make biochar a feasible option for widespread C sequestration endeavors.

The cost of biochar production plays a pivotal role in its marketing and application. When biochar is the primary product, its cost must cover operating expenses such as production, maintenance, feedstock, transport, labor, distribution, and other costs to ensure long-term business sustainability [159]. In some cases, biochar may be a by-product derived from processes aimed at enhancing existing agricultural or land management operations, as well as heating systems. Currently, there is no significant industrial biochar market that provides comprehensive data on biochar prices and costs. Market prices of biochar have been reported by commercial companies either based on mass or volume. Globally, the average price for biochar was \$2.65 per kg, ranging from as low as \$0.09 per kg in the Philippines to as high as \$8.85 per kg in the UK [159]. For blended biochars, the mean price was \$3.29 per kg, with a range of \$0.08 per kg in India to \$13.48 per kg in the US [159]. Thus, the market price of biochars exhibits significant variability depending on the origin of biochar production sites [160]. The collection of current biochar prices involved gathering data from companies across different countries and converting them to US dollars per kg. The dataset included 14 data points on commercial biochar prices, which ranged from \$0.8 to \$18 per kg [159]. Interestingly, the literature sources reported significantly lower prices, as low as \$0.05 per kg, but these values were excluded from the study. Based on the available data, the average cost of biochar was estimated to be around \$5.0 per kg [144]. However, to gain a deeper understanding of the pricing dynamics, it is necessary to conduct further investigations into the specific types of biochar and the distribution of price points.

Biochar-based carbon management networks (CMNs) provide a promising solution to achieve negative net GHG emissions [161]. These networks capitalize on established technologies for biochar production, distribution, and application, specifically through tillage practices. This makes them particularly advantageous for scaling up biochar utilization in agriculture-intensive economies, especially in developing countries. By incorporating biochar into existing agricultural systems, CMNs offer a viable pathway towards near-term GHG emissions reduction and contribute to sustainable climate change mitigation efforts [160]. To optimize the characteristics and applications of biochar, it is essential to select appropriate feedstocks and related biochar properties that align with specific applications [23,26].

The effectiveness of biochar-based negative emissions technologies heavily relies on our capacity to precisely forecast, optimize, and track the real climate change mitigation advantages [161]. To achieve maximum GHG reductions while minimizing any potential negative environmental consequences, computer-aided planning of biochar-based carbon management networks (CMNs) becomes crucial [161]. By integrating biochar applications into CMNs, which function as integrated systems akin to existing agro-industrial supply chains, the benefits of biochar on the soil can be optimized to enhance carbon stocks. According to Woolf et al. (2010), biochar-based CMNs have the potential to reduce emissions by a substantial 130 Gt CO₂ eq until 2100. The study suggests that approximately 60% of this reduction is attributed to direct carbon storage, while the remaining contribution arises from the beneficial secondary effects previously mentioned [162]. However, it is important to note that this estimate represents an optimistic upper limit and may not fully account for local conditions that could impose limitations on the utilization of biochar. Thus, further research is needed to assess the practical implications and potential challenges associated with implementing biochar-based CMNs in specific contexts. Conversely, McLaren estimated the annual emissions reduction potential of biochar-based CMNs to be 0.9–3.0 Gt CO₂ per year, with costs ranging from \$8 to \$300 per ton of CO₂ [163]. Such models can

assist decision-makers in understanding and optimizing the cost-benefit aspects of these systems to expedite their commercial deployment.

4.3. Carbon Stability and Persistence

While biochar is recognized for its capacity to sequester C over extended periods, the stability and persistence of C within biochar-amended soils can exhibit variability influenced by soil conditions, climate, and biochar characteristics. Maximizing the long-term stability of sequestered C is essential to optimize the effectiveness of biochar as a C mitigation strategy.

A recent investigation conducted in Belgium discovered arable fields ($n = 5$) featuring charcoal-enriched black spots ($>50 \text{ m}^2$; $n = 14$) that date back to over 150 years ago from historical charcoal production mound kilns [164]. Isotope analysis of the soil indicated that the maize-derived C concentration was significantly greater in charcoal-amended samples (0.44%) compared to the unamended neighboring soils (0.31%, $p = 0.02$) [164]. Over a 130-day period, it was observed that the C emissions from soils applied with maize-derived biochars significantly decreased by approximately half ($p < 0.02$). Stable C was found to be proportionally more present in protected soil aggregates in the presence of biochar [164]. The reduced specific mineralization and enhanced sequestration of recent C associated with biochar can be attributed to a combination of physical protection, microbial community C saturation, and potentially marginally higher annual primary production [111,138,163]. Altogether, this study provides compelling evidence of biochar's potential to enhance long-term C sequestration in soils by reducing C turnover.

Numerous studies have indicated that biochar-C stabilization occurs swiftly at high pyrolysis temperatures due to the interaction with variable charge minerals in the soil. For instance, an incubation experiment assessing MRTs of woody biochars revealed that the biochar pyrolyzed at $450 \text{ }^\circ\text{C}$ exhibited an MRT of 44 years, while the biochar pyrolyzed at $550 \text{ }^\circ\text{C}$ had an MRT of 610 years [141]. However, it is important to recognize that the effects of biochar on soil C sequestration cannot be uniformly generalized, as they depend on specific biochar properties, plant interactions, and site conditions. Currently, no meta-analyses have been reported that comprehensively analyze the impacts of biochar on soil C sequestration. For climate change mitigation through C sequestration to be effective, there must be a net removal of C from the atmosphere and its long-term storage in soil for several centuries to millennia. Deeper soil layers exhibit SOC with extended turnover times, enhanced stabilization mechanisms, and reduced susceptibility to decomposition and erosion. Interestingly, certain studies have even observed preferential accumulation of biochar C at greater depths over the long term. Therefore, it is hypothesized that surface application of biochar C (1) should be able to migrate to subsoil layers and (2) contribute to the deepening of SOC distribution, thereby making a notable contribution to climate change mitigation. To advance our understanding, detailed investigations are required to elucidate the mechanisms by which surface-applied biochar can be transported to deeper soil depths and how its application influences the input of organic C to these lower layers. Armed with this knowledge, biochar systems can be intentionally designed to maximize climate change mitigation through SOC sequestration.

4.4. Soil and Environmental Interactions

Biochar application can affect soil properties, nutrient dynamics, and microbial communities. However, the effects of biochar on these factors are intricate and multifaceted, with significant variability depending on various factors such as soil type, climate conditions, and specific biochar characteristics.

Numerous studies have been conducted to explore these aspects, shedding light on the complex relationship between biochar and soil processes. It has been observed that different soil types can display distinct responses to biochar amendments. For example, a study investigated the effects of biochar on soil greenhouse gas emissions across diverse soil types and revealed that biochar application significantly reduced nitrous oxide

emissions in sandy soil, whereas no significant effect was observed in clay soil [21]. This indicates that soil texture and composition play a pivotal role in determining the effectiveness of biochar in mitigating greenhouse gas emissions. Additionally, climate conditions play a crucial role in shaping the interactions between biochar and soil processes. A global meta-analysis was conducted to evaluate the effects of biochar on soil C dynamics in different climatic regions. Their research demonstrated that biochar application resulted in greater C sequestration in tropical soils compared to temperate soils [165]. The variation was attributed to disparities in microbial activity and temperature sensitivity between different regions [165].

These studies exemplify the intricate and context-dependent nature of biochar-soil interactions, highlighting the importance of considering soil type, climate conditions, and specific biochar properties when assessing the impacts of biochar on C sequestration and related factors. Understanding these complex interactions and their implications for ecosystem functioning is essential to mitigate potential negative consequences and optimize the benefits of biochar application. By taking into account the intricacies of soil type, climate conditions, and specific biochar characteristics, researchers and practitioners can make informed decisions and design sustainable biochar management strategies.

4.5. Regulatory Frameworks and Policy Support

The successful adoption of biochar as a C sequestration strategy necessitates the establishment of supportive regulatory frameworks and policies. Clear guidelines, standards, and incentives are crucial in promoting sustainable biochar production and facilitating its widespread utilization in C sequestration efforts. Developing robust policies can help address existing barriers and create an enabling environment for the effective application of biochar.

Several studies and literature sources emphasize the significance of regulatory frameworks and policies in promoting the use of biochar for C sequestration. For instance, a report prepared by the Natural Resources Defense Council in the United States highlighted the importance of supportive policies in overcoming market barriers and stimulating the production and utilization of biochar [166]. They argue that policies addressing issues such as quality standards, product labeling, and certification can enhance market confidence and promote the adoption of biochar in C sequestration initiatives. Similarly, Pourhashem et al. (2019) emphasize the role of policy frameworks in providing clear guidelines for sustainable biochar production and ensuring its environmental and agronomic benefits [167]. They suggest that policies should incentivize biochar use through mechanisms such as C credits, tax incentives, and subsidies [167].

Additionally, guidelines and standards play a vital role in ensuring the quality, safety, and efficacy of biochar products. The International Biochar Initiative (IBI) has developed guidelines for biochar production, utilization, and quality assessment, which serve as a valuable resource for industry stakeholders and policymakers [168]. These guidelines provide a framework for sustainable biochar production practices and help establish consistency and credibility in the biochar market.

Furthermore, incentives are essential for encouraging the adoption of biochar as a C sequestration strategy. Financial incentives, such as grants and subsidies, can support research and development, promote technology transfer, and incentivize the implementation of biochar projects [167]. Economic instruments like C pricing mechanisms, such as C taxes or cap-and-trade systems, can also create a market demand for biochar as a C offsetting tool [114].

By referencing and integrating these studies and viewpoints into policy discussions and decision-making processes, policymakers and stakeholders can develop comprehensive regulatory frameworks that facilitate the sustainable production and utilization of biochar for C sequestration.

4.6. Knowledge and Technology Transfer

The successful implementation of biochar applications for C sequestration necessitates extensive knowledge dissemination, technology transfer, and capacity building among various stakeholders. Educating farmers, land managers, and policymakers about the benefits, limitations, and best practices associated with biochar use is crucial for the widespread adoption of biochar as a C sequestration tool. Ensuring effective knowledge transfer can empower stakeholders to make informed decisions and maximize the potential benefits of biochar.

Numerous studies and literature sources highlight the importance of knowledge dissemination and capacity building in promoting the use of biochar for C sequestration. For instance, Guo et al. (2016) emphasize the need for education and outreach programs to communicate the advantages and limitations of biochar use to farmers and land managers [169]. They argue that providing technical guidance and training opportunities can facilitate the integration of biochar into agricultural practices [169]. Similarly, Campbell et al. (2018) stress the importance of knowledge dissemination to policymakers and stakeholders to ensure informed decision-making regarding biochar implementation [169]. They propose that comprehensive information on biochar properties, applications, and potential environmental and socioeconomic impacts should be made available to policymakers to support policy development and regulatory decision-making [169].

In addition to knowledge dissemination, effective technology transfer plays a vital role in facilitating the adoption of biochar applications. Farmers and land managers need access to appropriate and cost-effective biochar production technologies. Training programs, workshops, and demonstrations can provide hands-on experience and technical guidance for biochar production, application, and management. Capacity-building efforts should also focus on the establishment of monitoring and assessment protocols to evaluate the effectiveness of biochar applications in C sequestration. This can involve the development of standardized methodologies for measuring C sequestration, nutrient dynamics, and other relevant parameters [168]. Training programs and workshops that equip researchers and practitioners with the necessary skills and tools for monitoring and evaluating biochar effects are essential for building capacity in this field.

By integrating these perspectives into knowledge dissemination strategies and capacity-building initiatives, stakeholders can enhance their understanding of biochar applications, overcome potential barriers, and make informed decisions regarding the implementation of biochar for C sequestration.

5. Conclusions

Biochar holds promise as a valuable tool for soil C sequestration. Its potential to improve soil properties, enhance C storage, and mitigate greenhouse gas emissions is evident. However, to fully realize this potential, further research is needed to better understand the complex interactions between biochar and soil processes and to develop sustainable practices for its production and application. The stability and persistence of C within biochar-amended soils, although dependent on various factors, show potential for long-term C sequestration. The complex interactions between biochar and soil processes, influenced by soil type, climate conditions, and specific biochar characteristics, highlight the need for context-specific assessments. With appropriate policies, knowledge dissemination, and capacity building, biochar can play a significant role in addressing climate change and promoting sustainable land management practices.

Author Contributions: Conceptualization, S.L. and D.T.; methodology, S.L.; software, S.L.; validation, S.L. and D.T.; formal analysis, S.L.; investigation, S.L. and D.T.; resources, S.L.; data curation, S.L.; writing—original draft preparation, S.L. and D.T.; writing—review and editing, S.L.; visualization, S.L.; supervision, S.L.; project administration, S.L.; funding acquisition, S.L. All authors have read and agreed to the published version of the manuscript.

Funding: This research was funded by the United States Department of Agriculture—National Institute of Food and Agriculture (USDA-NIFA), grant number 2020-38422-32253.

Data Availability Statement: The data presented in this study are available upon request.

Acknowledgments: The authors would like to express their gratitude for the financial support from USDA-NIFA and the administrative support from Cal Poly Pomona Foundation, Inc.

Conflicts of Interest: The authors declare no conflict of interest. The funders had no role in the design of the study; in the collection, analyses, or interpretation of data; in the writing of the manuscript; or in the decision to publish the results.

References

1. Morecroft, M.D.; Duffield, S.; Harley, M.; Pearce-Higgins, J.W.; Stevens, N.; Watts, O.; Whitaker, J. Measuring the success of climate change adaptation and mitigation in terrestrial ecosystems. *Science* **2019**, *366*, eaaw9256. [[CrossRef](#)] [[PubMed](#)]
2. Sippel, S.; Meinshausen, N.; Fischer, E.M.; Székely, E.; Knutti, R. Climate change now detectable from any single day of weather at global scale. *Nat. Clim. Change* **2020**, *10*, 35–41. [[CrossRef](#)]
3. Tanner, T.; Lewis, D.; Wrathall, D.; Bronen, R.; Craddock-Henry, N.; Huq, S.; Lawless, C.; Nawrotzki, R.; Prasad, V.; Rahman, M.A. Livelihood resilience in the face of climate change. *Nat. Clim. Change* **2015**, *5*, 23–26. [[CrossRef](#)]
4. Yoro, K.O.; Daramola, M.O. CO₂ emission sources, greenhouse gases, and the global warming effect. In *Advances in Carbon Capture*; Elsevier: Amsterdam, The Netherlands, 2020; pp. 3–28.
5. Zheng, X.; Streimikiene, D.; Balezentis, T.; Mardani, A.; Cavallaro, F.; Liao, H. A review of greenhouse gas emission profiles, dynamics, and climate change mitigation efforts across the key climate change players. *J. Clean. Prod.* **2019**, *234*, 1113–1133. [[CrossRef](#)]
6. Driga, A.M.; Drigas, A.S. Climate Change 101: How Everyday Activities Contribute to the Ever-Growing Issue. *Int. J. Recent Contrib. Eng. Sci. IT* **2019**, *7*, 22–31. [[CrossRef](#)]
7. Gatti, L.V.; Basso, L.S.; Miller, J.B.; Gloor, M.; Gatti Domingues, L.; Cassol, H.L.; Tejada, G.; Aragão, L.E.; Nobre, C.; Peters, W. Amazonia as a carbon source linked to deforestation and climate change. *Nature* **2021**, *595*, 388–393. [[CrossRef](#)]
8. Seager, R.; Cane, M.; Henderson, N.; Lee, D.-E.; Abernathey, R.; Zhang, H. Strengthening tropical Pacific zonal sea surface temperature gradient consistent with rising greenhouse gases. *Nat. Clim. Change* **2019**, *9*, 517–522. [[CrossRef](#)]
9. Friedlingstein, P.; Jones, M.W.; O’Sullivan, M.; Andrew, R.M.; Bakker, D.C.; Hauck, J.; Le Quéré, C.; Peters, G.P.; Peters, W.; Pongratz, J. Global carbon budget 2021. *Earth Syst. Sci. Data* **2022**, *14*, 1917–2005. [[CrossRef](#)]
10. Mahato, M.; Nam, S.; Tabassian, R.; Oh, S.; Nguyen, V.H.; Oh, I.-K. Electronically Conjugated Multifunctional Covalent Triazine Framework for Unprecedented CO₂ Selectivity and High-Power Flexible Supercapacitor. *Adv. Funct. Mater.* **2022**, *32*, 2107442. [[CrossRef](#)]
11. Chen, J.; Elsgaard, L.; van Groenigen, K.J.; Olesen, J.E.; Liang, Z.; Jiang, Y.; Lærke, P.E.; Zhang, Y.; Luo, Y.; Hungate, B.A. Soil carbon loss with warming: New evidence from carbon-degrading enzymes. *Glob. Change Biol.* **2020**, *26*, 1944–1952. [[CrossRef](#)]
12. Soong, J.L.; Castanha, C.; Hicks Pries, C.E.; Ofiti, N.; Porras, R.C.; Riley, W.J.; Schmidt, M.W.; Torn, M.S. Five years of whole-soil warming led to loss of subsoil carbon stocks and increased CO₂ efflux. *Sci. Adv.* **2021**, *7*, eabd1343. [[CrossRef](#)] [[PubMed](#)]
13. Sun, W.; Canadell, J.G.; Yu, L.; Yu, L.; Zhang, W.; Smith, P.; Fischer, T.; Huang, Y. Climate drives global soil carbon sequestration and crop yield changes under conservation agriculture. *Glob. Change Biol.* **2020**, *26*, 3325–3335. [[CrossRef](#)] [[PubMed](#)]
14. van Dijk, M.; Morley, T.; Rau, M.L.; Saghay, Y. A meta-analysis of projected global food demand and population at risk of hunger for the period 2010–2050. *Nat. Food* **2021**, *2*, 494–501. [[CrossRef](#)] [[PubMed](#)]
15. Jacobson, T.A.; Kler, J.S.; Hernke, M.T.; Braun, R.K.; Meyer, K.C.; Funk, W.E. Direct human health risks of increased atmospheric carbon dioxide. *Nat. Sustain.* **2019**, *2*, 691–701. [[CrossRef](#)]
16. Chagas, J.K.M.; de Figueiredo, C.C.; Ramos, M.L.G. Biochar increases soil carbon pools: Evidence from a global meta-analysis. *J. Environ. Manag.* **2022**, *305*, 114403. [[CrossRef](#)] [[PubMed](#)]
17. Liao, W.; Thomas, S.C. Biochar particle size and post-pyrolysis mechanical processing affect soil pH, water retention capacity, and plant performance. *Soil Syst.* **2019**, *3*, 14. [[CrossRef](#)]
18. Kuz'yakov, Y.; Bogomolova, I.; Glaser, B. Biochar stability in soil: Decomposition during eight years and transformation as assessed by compound-specific ¹⁴C analysis. *Soil Biol. Biochem.* **2014**, *70*, 229–236. [[CrossRef](#)]
19. Fang, Y.; Singh, B.; Singh, B.P. Effect of temperature on biochar priming effects and its stability in soils. *Soil Biol. Biochem.* **2015**, *80*, 136–145. [[CrossRef](#)]
20. Li, S.; Skelly, S. Physicochemical properties and applications of biochars derived from municipal solid waste: A review. *Environ. Adv.* **2023**, *13*, 100395. [[CrossRef](#)]
21. Wu, D.; Senbayram, M.; Zang, H.; Ugurlar, F.; Aydemir, S.; Brüggemann, N.; Kuzyakov, Y.; Bol, R.; Blagodatskaya, E. Effect of biochar origin and soil pH on greenhouse gas emissions from sandy and clay soils. *Appl. Soil Ecol.* **2018**, *129*, 121–127. [[CrossRef](#)]
22. Dai, Z.; Xiong, X.; Zhu, H.; Xu, H.; Leng, P.; Li, J.; Tang, C.; Xu, J. Association of biochar properties with changes in soil bacterial, fungal and fauna communities and nutrient cycling processes. *Biochar* **2021**, *3*, 239–254. [[CrossRef](#)]

23. Wang, R.; Duan, X.; Wang, S.; Ren, N.-q.; Ho, S.-H. Production, properties, and catalytic applications of sludge derived biochar for environmental remediation. *Water Res.* **2020**, *187*, 116390.
24. Li, S.; Chan, C.Y. Will Biochar Suppress or Stimulate Greenhouse Gas Emissions in Agricultural Fields? Unveiling the Dice Game through Data Syntheses. *Soil Syst.* **2022**, *6*, 73. [[CrossRef](#)]
25. Elkhilfi, Z.; Iftikhar, J.; Sarraf, M.; Ali, B.; Saleem, M.H.; Ibranshabib, I.; Bispo, M.D.; Meili, L.; Ercisli, S.; Torun Kayabasi, E. Potential role of biochar on capturing soil nutrients, carbon sequestration and managing environmental challenges: A review. *Sustainability* **2023**, *15*, 2527. [[CrossRef](#)]
26. Mona, S.; Malyan, S.K.; Saini, N.; Deepak, B.; Pugazhendhi, A.; Kumar, S.S. Towards sustainable agriculture with carbon sequestration, and greenhouse gas mitigation using algal biochar. *Chemosphere* **2021**, *275*, 129856. [[CrossRef](#)] [[PubMed](#)]
27. Li, S.; Harris, S.; Anandhi, A.; Chen, G. Predicting biochar properties and functions based on feedstock and pyrolysis temperature: A review and data syntheses. *J. Clean. Prod.* **2019**, *215*, 890–902. [[CrossRef](#)]
28. Fazzalari, A.; Abou-Zaid, M.; Briens, C.; Briens, L. Impact of post-pyrolysis wash on biochar properties. *Can. J. Chem. Eng.* **2023**, *101*, 782–796. [[CrossRef](#)]
29. Singh, H.; Northup, B.K.; Rice, C.W.; Prasad, P.V. Biochar applications influence soil physical and chemical properties, microbial diversity, and crop productivity: A meta-analysis. *Biochar* **2022**, *4*, 8. [[CrossRef](#)]
30. Vetter, S.H.; Abdalla, M.; Kuhnert, M.; Smith, P. Soil Carbon Sequestration and Biochar. *Greenh. Gas Remov. Technol.* **2022**, *31*, 194.
31. Weng, Z.; Van Zwieten, L.; Tavakkoli, E.; Rose, M.T.; Singh, B.P.; Joseph, S.; Macdonald, L.M.; Kimber, S.; Morris, S.; Rose, T.J. Microspectroscopic visualization of how biochar lifts the soil organic carbon ceiling. *Nat. Commun.* **2022**, *13*, 5177. [[CrossRef](#)]
32. Situ, G.; Zhao, Y.; Zhang, L.; Yang, X.; Chen, D.; Li, S.; Wu, Q.; Xu, Q.; Chen, J.; Qin, H. Linking the chemical nature of soil organic carbon and biological binding agent in aggregates to soil aggregate stability following biochar amendment in a rice paddy. *Sci. Total Environ.* **2022**, *847*, 157460. [[CrossRef](#)] [[PubMed](#)]
33. Li, S.; Chen, G. Thermogravimetric, thermochemical, and infrared spectral characterization of feedstocks and biochar derived at different pyrolysis temperatures. *Waste Manag.* **2018**, *78*, 198–207. [[CrossRef](#)] [[PubMed](#)]
34. Li, S.; Barreto, V.; Li, R.; Chen, G.; Hsieh, Y.P. Nitrogen retention of biochar derived from different feedstocks at variable pyrolysis temperatures. *J. Anal. Appl. Pyrolysis* **2018**, *133*, 136–146. [[CrossRef](#)]
35. Sadaka, S.; Sharara, M.A.; Ashworth, A.; Keyser, P.; Allen, F.; Wright, A. Characterization of Biochar from Switchgrass Carbonization. *Energies* **2014**, *7*, 548–567. [[CrossRef](#)]
36. Muhammad, N.; Ge, L.; Chan, W.P.; Khan, A.; Nafees, M.; Lisak, G. Impacts of pyrolysis temperatures on physicochemical and structural properties of green waste derived biochars for adsorption of potentially toxic elements. *J. Environ. Manag.* **2022**, *317*, 115385. [[CrossRef](#)] [[PubMed](#)]
37. Hossain, M.K.; Strezov, V.; Chan, K.Y.; Ziolkowski, A.; Nelson, P.F. Influence of pyrolysis temperature on production and nutrient properties of wastewater sludge biochar. *J. Environ. Manag.* **2011**, *92*, 223–228. [[CrossRef](#)] [[PubMed](#)]
38. Ho, S.-H.; Yang, Z.-k.; Nagarajan, D.; Chang, J.-S.; Ren, N.-q. High-efficiency removal of lead from wastewater by biochar derived from anaerobic digestion sludge. *Bioresour. Technol.* **2017**, *246*, 142–149. [[CrossRef](#)]
39. Januševičius, T.; Mažeikienė, A.; Danila, V.; Paliulis, D. The characteristics of sewage sludge pellet biochar prepared using two different pyrolysis methods. *Biomass Convers. Bioref.* **2022**. [[CrossRef](#)]
40. Devi, P.; Saroha, A.K. Effect of pyrolysis temperature on polycyclic aromatic hydrocarbons toxicity and sorption behaviour of biochars prepared by pyrolysis of paper mill effluent treatment plant sludge. *Bioresour. Technol.* **2015**, *192*, 312–320. [[CrossRef](#)]
41. Zhang, H.; Chen, C.; Gray, E.M.; Boyd, S.E. Effect of feedstock and pyrolysis temperature on properties of biochar governing end use efficacy. *Biomass Bioenergy* **2017**, *105*, 136–146. [[CrossRef](#)]
42. Takaya, C.A.; Fletcher, L.A.; Singh, S.; Anyikude, K.U.; Ross, A.B. Phosphate and ammonium sorption capacity of biochar and hydrochar from different wastes. *Chemosphere* **2016**, *145*, 518–527. [[CrossRef](#)] [[PubMed](#)]
43. Al-Wabel, M.I.; Al-Omran, A.; El-Naggar, A.H.; Nadeem, M.; Usman, A.R.A. Pyrolysis temperature induced changes in characteristics and chemical composition of biochar produced from conocarpus wastes. *Bioresour. Technol.* **2013**, *131*, 374–379. [[CrossRef](#)] [[PubMed](#)]
44. Almutairi, A.A.; Ahmad, M.; Rafique, M.I.; Al-Wabel, M.I. Variations in composition and stability of biochars derived from different feedstock types at varying pyrolysis temperature. *J. Saudi Soc. Agric. Sci.* **2023**, *22*, 25–34. [[CrossRef](#)]
45. Behnam, H.; Firouzi, A.F. Effects of synthesis method, feedstock type, and pyrolysis temperature on physicochemical properties of biochar nanoparticles. *Biomass Convers. Bioref.* **2022**. [[CrossRef](#)]
46. Wang, S.; Gao, B.; Zimmerman, A.R.; Li, Y.; Ma, L.; Harris, W.G.; Migliaccio, K.W. Physicochemical and sorptive properties of biochars derived from woody and herbaceous biomass. *Chemosphere* **2015**, *134*, 257–262. [[CrossRef](#)] [[PubMed](#)]
47. Chen, T.; Zhang, Y.; Wang, H.; Lu, W.; Zhou, Z.; Zhang, Y.; Ren, L. Influence of pyrolysis temperature on characteristics and heavy metal adsorptive performance of biochar derived from municipal sewage sludge. *Bioresour. Technol.* **2014**, *164*, 47–54. [[CrossRef](#)]
48. Zielińska, A.; Oleszczuk, P.; Charmas, B.; Skubiszewska-Zięba, J.; Pasieczna-Patkowska, S. Effect of sewage sludge properties on the biochar characteristic. *J. Anal. Appl. Pyrolysis* **2015**, *112*, 201–213. [[CrossRef](#)]
49. Li, L.; Long, A.; Fossum, B.; Kaiser, M. Effects of pyrolysis temperature and feedstock type on biochar characteristics pertinent to soil carbon and soil health: A meta-analysis. *Soil Use Manag.* **2023**, *39*, 43–52. [[CrossRef](#)]
50. Tomczyk, A.; Sokołowska, Z.; Boguta, P. Biochar physicochemical properties: Pyrolysis temperature and feedstock kind effects. *Rev. Environ. Sci. Bio/Technol.* **2020**, *19*, 191–215. [[CrossRef](#)]

51. Picchio, R.; Latterini, F.; Venanzi, R.; Stefanoni, W.; Suardi, A.; Tocci, D.; Pari, L. Pellet production from woody and non-woody feedstocks: A review on biomass quality evaluation. *Energies* **2020**, *13*, 2937. [[CrossRef](#)]
52. Janu, R.; Mrlik, V.; Ribitsch, D.; Hofman, J.; Sedláček, P.; Bielská, L.; Soja, G. Biochar surface functional groups as affected by biomass feedstock, biochar composition and pyrolysis temperature. *Carbon Resour. Convers.* **2021**, *4*, 36–46. [[CrossRef](#)]
53. Brickler, C.A.; Wu, Y.; Li, S.; Anandhi, A.; Chen, G. Comparing Physicochemical Properties and Sorption Behaviors of Pyrolysis-Derived and Microwave-Mediated Biochar. *Sustainability* **2021**, *13*, 2359. [[CrossRef](#)]
54. Ippolito, J.A.; Cui, L.; Kammann, C.; Wrage-Mönning, N.; Estavillo, J.M.; Fuertes-Mendizabal, T.; Cayuela, M.L.; Sigua, G.; Novak, J.; Spokas, K. Feedstock choice, pyrolysis temperature and type influence biochar characteristics: A comprehensive meta-data analysis review. *Biochar* **2020**, *2*, 421–438. [[CrossRef](#)]
55. Ma, S.; Wang, X.; Wang, S.; Feng, K. Effects of temperature on physicochemical properties of rice straw biochar and its passivation ability to Cu²⁺ in soil. *J. Soils Sediments* **2022**, *22*, 1418–1430. [[CrossRef](#)]
56. Xu, Z.; He, M.; Xu, X.; Cao, X.; Tsang, D.C. Impacts of different activation processes on the carbon stability of biochar for oxidation resistance. *Bioresour. Technol.* **2021**, *338*, 125555. [[CrossRef](#)]
57. Leng, L.; Huang, H.; Li, H.; Li, J.; Zhou, W. Biochar stability assessment methods: A review. *Sci. Total Environ.* **2019**, *647*, 210–222. [[CrossRef](#)]
58. Han, L.; Ro, K.S.; Wang, Y.; Sun, K.; Sun, H.; Libra, J.A.; Xing, B. Oxidation resistance of biochars as a function of feedstock and pyrolysis condition. *Sci. Total Environ.* **2018**, *616*, 335–344. [[CrossRef](#)]
59. Wani, L.; Sharma, A.; Kushvaha, V.; Madhushri, P.; Peng, L. Effect of pH, volatile content, and pyrolysis conditions on surface area and O/C and H/C ratios of biochar: Towards understanding performance of biochar using simplified approach. *J. Hazard. Toxic Radioact. Waste* **2020**, *24*, 04020048. [[CrossRef](#)]
60. Zhang, H.; Liao, W.; Zhou, X.; Shao, J.; Chen, Y.; Zhang, S.; Chen, H. Coeffect of pyrolysis temperature and potassium phosphate impregnation on characteristics, stability, and adsorption mechanism of phosphorus-enriched biochar. *Bioresour. Technol.* **2022**, *344*, 126273. [[CrossRef](#)]
61. Spokas, K.A. Review of the stability of biochar in soils: Predictability of O:C molar ratios. *Carbon Manag.* **2010**, *1*, 289–303. [[CrossRef](#)]
62. Krysanova, K.; Krylova, A.; Zaichenko, V. Properties of biochar obtained by hydrothermal carbonization and torrefaction of peat. *Fuel* **2019**, *256*, 115929. [[CrossRef](#)]
63. Zhang, C.; Ho, S.-H.; Chen, W.-H.; Fu, Y.; Chang, J.-S.; Bi, X. Oxidative torrefaction of biomass nutshells: Evaluations of energy efficiency as well as biochar transportation and storage. *Appl. Energy* **2019**, *235*, 428–441. [[CrossRef](#)]
64. Zhang, Y.; Qin, J.; Yi, Y. Biochar and hydrochar derived from freshwater sludge: Characterization and possible applications. *Sci. Total Environ.* **2021**, *763*, 144550. [[CrossRef](#)]
65. Bahcivanji, L.; Gasco, G.; Paz-Ferreiro, J.; Méndez, A. The effect of post-pyrolysis treatment on waste biomass derived hydrochar. *Waste Manag.* **2020**, *106*, 55–61. [[CrossRef](#)] [[PubMed](#)]
66. Amrullah, A.; Farobie, O.; Bayu, A.; Syaftika, N.; Hartulistiyoso, E.; Moheimani, N.R.; Karnjanakom, S.; Matsumura, Y. Slow pyrolysis of ulva lactuca (chlorophyta) for sustainable production of bio-oil and biochar. *Sustainability* **2022**, *14*, 3233. [[CrossRef](#)]
67. Wyn, H.K.; Zárate, S.; Carrascal, J.; Yermán, L. A novel approach to the production of biochar with improved fuel characteristics from biomass waste. *Waste Biomass Valoriz.* **2020**, *11*, 6467–6481. [[CrossRef](#)]
68. Nzediegwu, C.; Arshad, M.; Ulah, A.; Naeth, M.A.; Chang, S.X. Fuel, thermal and surface properties of microwave-pyrolyzed biochars depend on feedstock type and pyrolysis temperature. *Bioresour. Technol.* **2021**, *320*, 124282. [[CrossRef](#)]
69. Suman, S.; Gautam, S. Biochar derived from agricultural waste biomass act as a clean and alternative energy source of fossil fuel inputs. In *Energy Systems and Environment*; IntechOpen: London, UK, 2018; p. 207.
70. Ahmed, A.; Bakar, M.S.A.; Hamdani, R.; Park, Y.-K.; Lam, S.S.; Sukri, R.S.; Hussain, M.; Majeed, K.; Phusunti, N.; Jamil, F. Valorization of underutilized waste biomass from invasive species to produce biochar for energy and other value-added applications. *Environ. Res.* **2020**, *186*, 109596. [[CrossRef](#)]
71. Kwapinski, W.; Byrne, C.M.P.; Kryachko, E.; Wolfram, P.; Adley, C.; Leahy, J.J.; Novotny, E.H.; Hayes, M.H.B. Biochar from Biomass and Waste. *Waste Biomass Valoriz.* **2010**, *1*, 177–189. [[CrossRef](#)]
72. Enders, A.; Lehmann, J. Proximate analyses for characterising biochars. In *Biochar: A Guide to Analytical Methods*; CRC Press: Boca Raton, FL, USA, 2017; pp. 9–22.
73. Chen, J.; Wang, P.; Ding, L.; Yu, T.; Leng, S.; Chen, J.; Fan, L.; Li, J.; Wei, L.; Li, J.; et al. The comparison study of multiple biochar stability assessment methods. *J. Anal. Appl. Pyrolysis* **2021**, *156*, 105070. [[CrossRef](#)]
74. Klasson, K.T. Biochar characterization and a method for estimating biochar quality from proximate analysis results. *Biomass Bioenergy* **2017**, *96*, 50–58. [[CrossRef](#)]
75. Yi, L.; Feng, J.; Qin, Y.-H.; Li, W.-Y. Prediction of elemental composition of coal using proximate analysis. *Fuel* **2017**, *193*, 315–321. [[CrossRef](#)]
76. Pastorova, I.; Botto, R.E.; Arisz, P.W.; Boon, J.J. Cellulose char structure: A combined analytical Py-GC-MS, FTIR, and NMR study. *Carbohydr. Res.* **1994**, *262*, 27–47. [[CrossRef](#)]
77. Brebu, M.; Tamminen, T.; Spiridon, I. Thermal degradation of various lignins by TG-MS/FTIR and Py-GC-MS. *J. Anal. Appl. Pyrolysis* **2013**, *104*, 531–539. [[CrossRef](#)]

78. Ghysels, S.; Rathnayake, D.; Maziarka, P.; Mašek, O.; Sohi, S.; Ronsse, F. Biochar stability scores from analytical pyrolysis (Py-GC-MS). *J. Anal. Appl. Pyrolysis* **2022**, *161*, 105412. [[CrossRef](#)]
79. Conti, R.; Rombolà, A.G.; Modelli, A.; Torri, C.; Fabbri, D. Evaluation of the thermal and environmental stability of switchgrass biochars by Py-GC-MS. *J. Anal. Appl. Pyrolysis* **2014**, *110*, 239–247. [[CrossRef](#)]
80. Suárez-Abelenda, M.; Kaal, J.; McBeath, A.V. Translating analytical pyrolysis fingerprints to Thermal Stability Indices (TSI) to improve biochar characterization by pyrolysis-GC-MS. *Biomass Bioenergy* **2017**, *98*, 306–320. [[CrossRef](#)]
81. Challinor, J.M. The development and applications of thermally assisted hydrolysis and methylation reactions. *J. Anal. Appl. Pyrolysis* **2001**, *61*, 3–34. [[CrossRef](#)]
82. Zhang, T.; Wu, X.; Li, H.; Tsang, D.C.; Li, G.; Ren, H. Struvite pyrolysate cycling technology assisted by thermal hydrolysis pretreatment to recover ammonium nitrogen from composting leachate. *J. Clean. Prod.* **2020**, *242*, 118442. [[CrossRef](#)]
83. van Keulen, H.; Schilling, M. AMDIS & EXCEL: A powerful combination for evaluating THM-Py-GC/MS results from European lacquers. *Stud. Conserv.* **2019**, *64* (Suppl. S1), S74–S80.
84. Amusat, S.O.; Kebede, T.G.; Nxumalo, E.N.; Dube, S.; Nindi, M.M. Incorporating pristine biochar into metal-organic frameworks: Facile green synthesis, characterization, and wastewater remediation. *Bioresour. Technol. Rep.* **2022**, *19*, 101160. [[CrossRef](#)]
85. Harvey, O.R.; Kuo, L.-J.; Zimmerman, A.R.; Louchouart, P.; Amonette, J.E.; Herbert, B.E. An index-based approach to assessing recalcitrance and soil carbon sequestration potential of engineered black carbons (biochars). *Environ. Sci. Technol.* **2012**, *46*, 1415–1421. [[CrossRef](#)] [[PubMed](#)]
86. Windeatt, J.H.; Ross, A.B.; Williams, P.T.; Forster, P.M.; Nahil, M.A.; Singh, S. Characteristics of biochars from crop residues: Potential for carbon sequestration and soil amendment. *J. Environ. Manag.* **2014**, *146*, 189–197. [[CrossRef](#)] [[PubMed](#)]
87. Han, L.; Sun, H.; Sun, K.; Yang, Y.; Fang, L.; Xing, B. Effect of Fe and Al ions on the production of biochar from agricultural biomass: Properties, stability and adsorption efficiency of biochar. *Renew. Sustain. Energy Rev.* **2021**, *145*, 111133. [[CrossRef](#)]
88. Zhao, L.; Cao, X.; Mašek, O.; Zimmerman, A. Heterogeneity of biochar properties as a function of feedstock sources and production temperatures. *J. Hazard. Mater.* **2013**, *256*, 1–9. [[CrossRef](#)]
89. Gómez, N.; Rosas, J.G.; Singh, S.; Ross, A.B.; Sánchez, M.E.; Cara, J. Development of a gained stability index for describing biochar stability: Relation of high recalcitrance index (R50) with accelerated ageing tests. *J. Anal. Appl. Pyrolysis* **2016**, *120*, 37–44. [[CrossRef](#)]
90. Cross, A.; Sohi, S.P. A method for screening the relative long-term stability of biochar. *GCB Bioenergy* **2013**, *5*, 215–220. [[CrossRef](#)]
91. Hsieh, Y.-P. A novel multielemental scanning thermal analysis (MESTA) method for the identification and characterization of solid substances. *J. AOAC Int.* **2007**, *90*, 54–59. [[PubMed](#)]
92. Leng, L.; Huang, H. An overview of the effect of pyrolysis process parameters on biochar stability. *Bioresour. Technol.* **2018**, *270*, 627–642. [[CrossRef](#)]
93. Mašek, O.; Brownsort, P.; Cross, A.; Sohi, S. Influence of production conditions on the yield and environmental stability of biochar. *Fuel* **2013**, *103*, 151–155. [[CrossRef](#)]
94. Enders, A.; Hanley, K.; Whitman, T.; Joseph, S.; Lehmann, J. Characterization of biochars to evaluate recalcitrance and agronomic performance. *Bioresour. Technol.* **2012**, *114*, 644–653. [[CrossRef](#)]
95. Jindo, K.; Sonoki, T. Comparative assessment of biochar stability using multiple indicators. *Agronomy* **2019**, *9*, 254. [[CrossRef](#)]
96. Leng, L.; Xu, X.; Wei, L.; Fan, L.; Huang, H.; Li, J.; Lu, Q.; Li, J.; Zhou, W. Biochar stability assessment by incubation and modelling: Methods, drawbacks and recommendations. *Sci. Total Environ.* **2019**, *664*, 11–23. [[CrossRef](#)] [[PubMed](#)]
97. Wang, J.; Xiong, Z.; Kuzyakov, Y. Biochar stability in soil: Meta-analysis of decomposition and priming effects. *GCB Bioenergy* **2016**, *8*, 512–523. [[CrossRef](#)]
98. Weng, Z.; Van Zwieten, L.; Singh, B.P.; Tavakkoli, E.; Joseph, S.; Macdonald, L.M.; Rose, T.J.; Rose, M.T.; Kimber, S.W.; Morris, S. Biochar built soil carbon over a decade by stabilizing rhizodeposits. *Nat. Clim. Change* **2017**, *7*, 371–376. [[CrossRef](#)]
99. Liu, X.; Feng, P.; Zhang, X. Effect of biochar on soil aggregates in the Loess Plateau: Results from incubation experiments. *Int. J. Agric. Biol.* **2012**, *14*, 975–979.
100. Rechberger, M.V.; Kloss, S.; Rennhofer, H.; Tintner, J.; Watzinger, A.; Soja, G.; Lichtenegger, H.; Zehetner, F. Changes in biochar physical and chemical properties: Accelerated biochar aging in an acidic soil. *Carbon* **2017**, *115*, 209–219. [[CrossRef](#)]
101. Yao, R.; Li, H.; Zhu, W.; Yang, J.; Wang, X.; Yin, C.; Jing, Y.; Chen, Q.; Xie, W. Biochar and potassium humate shift the migration, transformation and redistribution of urea-N in salt-affected soil under drip fertigation: Soil column and incubation experiments. *Irrig. Sci.* **2022**, *40*, 267–282. [[CrossRef](#)]
102. Lehmann, J.; Joseph, S. *Biochar for Environmental Management: Science, Technology and Implementation*; Routledge: New York, NY, USA, 2015.
103. Rasse, D.P.; Budai, A.; O’Toole, A.; Ma, X.; Rumpel, C.; Abiven, S. Persistence in soil of Miscanthus biochar in laboratory and field conditions. *PLoS ONE* **2017**, *12*, e0184383. [[CrossRef](#)]
104. Singh, B.P.; Fang, Y.; Boersma, M.; Collins, D.; Van Zwieten, L.; Macdonald, L.M. In situ persistence and migration of biochar carbon and its impact on native carbon emission in contrasting soils under managed temperate pastures. *PLoS ONE* **2015**, *10*, e0141560. [[CrossRef](#)]
105. Weng, Z.H.; Liu, X.; Eldridge, S.; Wang, H.; Rose, T.; Rose, M.; Rust, J.; Singh, B.P.; Tavakkoli, E.; Tang, C. Priming of soil organic carbon induced by sugarcane residues and its biochar control the source of nitrogen for plant uptake: A dual ¹³C and ¹⁵N isotope three-source-partitioning study. *Soil Biol. Biochem.* **2020**, *146*, 107792. [[CrossRef](#)]

106. Budai, A.; Zimmerman, A.; Cowie, A.; Webber, J.; Singh, B.; Glaser, B.; Masiello, C.; Andersson, D.; Shields, F.; Lehmann, J. Biochar Carbon Stability Test Method: An assessment of methods to determine biochar carbon stability. *Int. Biochar Initiat.* **2013**, *20*, 1–10.
107. Deng, B.; Yuan, X.; Siemann, E.; Wang, S.; Fang, H.; Wang, B.; Gao, Y.; Shad, N.; Liu, X.; Zhang, W. Feedstock particle size and pyrolysis temperature regulate effects of biochar on soil nitrous oxide and carbon dioxide emissions. *Waste Manag.* **2021**, *120*, 33–40. [[CrossRef](#)] [[PubMed](#)]
108. Singh, N.; Kookana, R.S. Organo-mineral interactions mask the true sorption potential of biochars in soils. *J. Environ. Sci. Health Part B* **2009**, *44*, 214–219. [[CrossRef](#)] [[PubMed](#)]
109. Zhu, Y.; Yi, B.; Hu, H.; Zong, Z.; Chen, M.; Yuan, Q. The relationship of structure and organic matter adsorption characteristics by magnetic cattle manure biochar prepared at different pyrolysis temperatures. *J. Environ. Chem. Eng.* **2020**, *8*, 104112. [[CrossRef](#)]
110. Palansooriya, K.N.; Wong, J.T.F.; Hashimoto, Y.; Huang, L.; Rinklebe, J.; Chang, S.X.; Bolan, N.; Wang, H.; Ok, Y.S. Response of microbial communities to biochar-amended soils: A critical review. *Biochar* **2019**, *1*, 3–22. [[CrossRef](#)]
111. Lorenz, K.; Lal, R. Biochar application to soil for climate change mitigation by soil organic carbon sequestration. *J. Plant Nutr. Soil Sci.* **2014**, *177*, 651–670. [[CrossRef](#)]
112. Jatav, H.S.; Rajput, V.D.; Minkina, T.; Singh, S.K.; Chejara, S.; Gorovtsov, A.; Barakhov, A.; Bauer, T.; Sushkova, S.; Mandzhieva, S. Sustainable approach and safe use of biochar and its possible consequences. *Sustainability* **2021**, *13*, 10362. [[CrossRef](#)]
113. Ameloot, N.; Sleutel, S.; Case, S.D.C.; Alberti, G.; McNamara, N.P.; Zavalloni, C.; Vervisch, B.; Vedove, G.d.; De Neve, S. C mineralization and microbial activity in four biochar field experiments several years after incorporation. *Soil Biol. Biochem.* **2014**, *78*, 195–203. [[CrossRef](#)]
114. Ameloot, N.; Graber, E.R.; Verheijen, F.G.; De Neve, S. Interactions between biochar stability and soil organisms: Review and research needs. *Eur. J. Soil Sci.* **2013**, *64*, 379–390. [[CrossRef](#)]
115. Memetova, A.; Tyagi, I.; Karri, R.R.; Kumar, V.; Tyagi, K.; Suhas; Memetov, N.; Zelenin, A.; Pasko, T.; Gerasimova, A.; et al. Porous carbon-based material as a sustainable alternative for the storage of natural gas (methane) and biogas (biomethane): A review. *Chem. Eng. J.* **2022**, *446*, 137373. [[CrossRef](#)]
116. Atkinson, C.J.; Fitzgerald, J.D.; Hippias, N.A. Potential mechanisms for achieving agricultural benefits from biochar application to temperate soils: A review. *Plant Soil* **2010**, *337*, 1–18. [[CrossRef](#)]
117. Jung, S.; Park, Y.-K.; Kwon, E.E. Strategic use of biochar for CO₂ capture and sequestration. *J. CO₂ Util.* **2019**, *32*, 128–139. [[CrossRef](#)]
118. Yazdani, M.R.; Duimovich, N.; Tiraferri, A.; Laurell, P.; Borghei, M.; Zimmerman, J.B.; Vahala, R. Tailored mesoporous biochar sorbents from pinecone biomass for the adsorption of natural organic matter from lake water. *J. Mol. Liq.* **2019**, *291*, 111248. [[CrossRef](#)]
119. Zhao, L.; Zheng, W.; Cao, X. Distribution and evolution of organic matter phases during biochar formation and their importance in carbon loss and pore structure. *Chem. Eng. J.* **2014**, *250*, 240–247. [[CrossRef](#)]
120. Zhang, Y.; Wang, S.; Feng, D.; Gao, J.; Dong, L.; Zhao, Y.; Sun, S.; Huang, Y.; Qin, Y. Functional Biochar Synergistic Solid/Liquid-Phase CO₂ Capture: A Review. *Energy Fuels* **2022**, *36*, 2945–2970. [[CrossRef](#)]
121. Prasad, M.; Tzortzakis, N.; McDaniel, N. Chemical characterization of biochar and assessment of the nutrient dynamics by means of preliminary plant growth tests. *J. Environ. Manag.* **2018**, *216*, 89–95. [[CrossRef](#)]
122. Domingues, R.R.; Sánchez-Monedero, M.A.; Spokas, K.A.; Melo, L.C.A.; Trugilho, P.F.; Valenciano, M.N.; Silva, C.A. Enhancing Cation Exchange Capacity of Weathered Soils Using Biochar: Feedstock, Pyrolysis Conditions and Addition Rate. *Agronomy* **2020**, *10*, 824. [[CrossRef](#)]
123. Khadem, A.; Raiesi, F.; Besharati, H.; Khalaj, M.A. The effects of biochar on soil nutrients status, microbial activity and carbon sequestration potential in two calcareous soils. *Biochar* **2021**, *3*, 105–116. [[CrossRef](#)]
124. Rogovska, N.; Laird, D.A.; Rathke, S.J.; Karlen, D.L. Biochar impact on Midwestern Mollisols and maize nutrient availability. *Geoderma* **2014**, *230–231*, 340–347. [[CrossRef](#)]
125. Madiba, O.F.; Solaiman, Z.M.; Carson, J.K.; Murphy, D.V. Biochar increases availability and uptake of phosphorus to wheat under leaching conditions. *Biol. Fertil. Soils* **2016**, *52*, 439–446. [[CrossRef](#)]
126. Palviainen, M.; Berninger, F.; Bruckman, V.J.; Köster, K.; de Assumpção, C.R.M.; Aaltonen, H.; Makita, N.; Mishra, A.; Kulmala, L.; Adamczyk, B.; et al. Effects of biochar on carbon and nitrogen fluxes in boreal forest soil. *Plant Soil* **2018**, *425*, 71–85. [[CrossRef](#)]
127. Kan, Z.-R.; Liu, Q.-Y.; Wu, G.; Ma, S.-T.; Virk, A.L.; Qi, J.-Y.; Zhao, X.; Zhang, H.-L. Temperature and moisture driven changes in soil carbon sequestration and mineralization under biochar addition. *J. Clean. Prod.* **2020**, *265*, 121921. [[CrossRef](#)]
128. Wang, L.; O'Connor, D.; Rinklebe, J.; Ok, Y.S.; Tsang, D.C.W.; Shen, Z.; Hou, D. Biochar Aging: Mechanisms, Physicochemical Changes, Assessment, And Implications for Field Applications. *Environ. Sci. Technol.* **2020**, *54*, 14797–14814. [[CrossRef](#)]
129. Li, Y.; Li, Y.; Chang, S.X.; Yang, Y.; Fu, S.; Jiang, P.; Luo, Y.; Yang, M.; Chen, Z.; Hu, S.; et al. Biochar reduces soil heterotrophic respiration in a subtropical plantation through increasing soil organic carbon recalcitrancy and decreasing carbon-degrading microbial activity. *Soil Biol. Biochem.* **2018**, *122*, 173–185. [[CrossRef](#)]
130. Chenu, C.; Angers, D.A.; Barré, P.; Derrien, D.; Arrouays, D.; Balesdent, J. Increasing organic stocks in agricultural soils: Knowledge gaps and potential innovations. *Soil Tillage Res.* **2019**, *188*, 41–52. [[CrossRef](#)]
131. Hu, F.; Xu, C.; Ma, R.; Tu, K.; Yang, J.; Zhao, S.; Yang, M.; Zhang, F. Biochar application driven change in soil internal forces improves aggregate stability: Based on a two-year field study. *Geoderma* **2021**, *403*, 115276. [[CrossRef](#)]

132. Kimetu, J.M.; Lehmann, J. Stability and stabilisation of biochar and green manure in soil with different organic carbon contents. *Soil Res.* **2010**, *48*, 577–585. [[CrossRef](#)]
133. Soinne, H.; Hovi, J.; Tammeorg, P.; Turtola, E. Effect of biochar on phosphorus sorption and clay soil aggregate stability. *Geoderma* **2014**, *219–220*, 162–167. [[CrossRef](#)]
134. Hu, F.; Liu, J.; Xu, C.; Du, W.; Yang, Z.; Liu, X.; Liu, G.; Zhao, S. Soil internal forces contribute more than raindrop impact force to rainfall splash erosion. *Geoderma* **2018**, *330*, 91–98. [[CrossRef](#)]
135. Pituello, C.; Dal Ferro, N.; Francioso, O.; Simonetti, G.; Berti, A.; Piccoli, I.; Pisi, A.; Morari, F. Effects of biochar on the dynamics of aggregate stability in clay and sandy loam soils. *Eur. J. Soil Sci.* **2018**, *69*, 827–842. [[CrossRef](#)]
136. Pei, J.; Li, J.; Fang, C.; Zhao, J.; Nie, M.; Wu, J. Different responses of root exudates to biochar application under elevated CO₂. *Agric. Ecosyst. Environ.* **2020**, *301*, 107061. [[CrossRef](#)]
137. Shi, S.; Zhang, Q.; Lou, Y.; Du, Z.; Wang, Q.; Hu, N.; Wang, Y.; Gunina, A.; Song, J. Soil organic and inorganic carbon sequestration by consecutive biochar application: Results from a decade field experiment. *Soil Use Manag.* **2021**, *37*, 95–103. [[CrossRef](#)]
138. Jaafar, N.M.; Clode, P.L.; Abbott, L.K. Microscopy observations of habitable space in biochar for colonization by fungal hyphae from soil. *J. Integr. Agric.* **2014**, *13*, 483–490. [[CrossRef](#)]
139. Zheng, H.; Liu, D.; Liao, X.; Miao, Y.; Li, Y.; Li, J.; Yuan, J.; Chen, Z.; Ding, W. Field-aged biochar enhances soil organic carbon by increasing recalcitrant organic carbon fractions and making microbial communities more conducive to carbon sequestration. *Agric. Ecosyst. Environ.* **2022**, *340*, 108177. [[CrossRef](#)]
140. Ghosh, D.; Maiti, S.K. Invasive weed-based biochar facilitated the restoration of coal mine degraded land by modulating the enzyme activity and carbon sequestration. *Restor. Ecol.* **2023**, *31*, e13744. [[CrossRef](#)]
141. Yin, Y.-f.; He, X.-h.; Ren, G.; Yang, Y.-s. Effects of rice straw and its biochar addition on soil labile carbon and soil organic carbon. *J. Integr. Agric.* **2014**, *13*, 491–498. [[CrossRef](#)]
142. Fang, Y.; Singh, B.; Singh, B.P.; Krull, E. Biochar carbon stability in four contrasting soils. *Eur. J. Soil Sci.* **2014**, *65*, 60–71. [[CrossRef](#)]
143. Xu, R.; Ferrante, L.; Hall, K.; Briens, C.; Berruti, F. Thermal self-sustainability of biochar production by pyrolysis. *J. Anal. Appl. Pyrolysis* **2011**, *91*, 55–66. [[CrossRef](#)]
144. Freddo, A.; Cai, C.; Reid, B.J. Environmental contextualisation of potential toxic elements and polycyclic aromatic hydrocarbons in biochar. *Environ. Pollut.* **2012**, *171*, 18–24. [[CrossRef](#)]
145. Terzano, R.; Rascio, I.; Allegretta, I.; Porfido, C.; Spagnuolo, M.; Khanghahi, M.Y.; Crecchio, C.; Sakellariadou, F.; Gattullo, C.E. Fire effects on the distribution and bioavailability of potentially toxic elements (PTEs) in agricultural soils. *Chemosphere* **2021**, *281*, 130752. [[CrossRef](#)] [[PubMed](#)]
146. Zhang, A.; Li, X.; Xing, J.; Xu, G. Adsorption of potentially toxic elements in water by modified biochar: A review. *J. Environ. Chem. Eng.* **2020**, *8*, 104196. [[CrossRef](#)]
147. Singh, P.; Sarswat, A.; Pittman, C.U., Jr.; Mlsna, T.; Mohan, D. Sustainable low-concentration arsenite [As (III)] removal in single and multicomponent systems using hybrid Iron oxide–biochar nanocomposite adsorbents—A mechanistic study. *ACS Omega* **2020**, *5*, 2575–2593. [[CrossRef](#)] [[PubMed](#)]
148. Liu, L.; Fan, L.; Jin, K.; Qian, J.; Huang, P.; Peng, H.; Zhou, W.; Chen, P.; Ruan, R. One-pot synthesis of lignin biochar supported Ni for catalytic pyrolysis of *Chlorella vulgaris* and its model compounds: The formation mechanism of aromatic hydrocarbons. *Fuel* **2023**, *341*, 127558. [[CrossRef](#)]
149. Wang, C.; Wang, Y.; Herath, H. Polycyclic aromatic hydrocarbons (PAHs) in biochar—Their formation, occurrence and analysis: A review. *Org. Geochem.* **2017**, *114*, 1–11. [[CrossRef](#)]
150. Keiluweit, M.; Kleber, M.; Sparrow, M.A.; Simoneit, B.R.; Prah, F.G. Solvent-extractable polycyclic aromatic hydrocarbons in biochar: Influence of pyrolysis temperature and feedstock. *Environ. Sci. Technol.* **2012**, *46*, 9333–9341. [[CrossRef](#)]
151. Buss, W.; Hilber, I.; Graham, M.C.; Mašek, O. Composition of PAHs in biochar and implications for biochar production. *ACS Sustain. Chem. Eng.* **2022**, *10*, 6755–6765. [[CrossRef](#)]
152. Ye, W.; Xu, X.; Zhan, M.; Huang, Q.; Li, X.; Jiao, W.; Yin, Y. Formation behavior of PAHs during pyrolysis of waste tires. *J. Hazard. Mater.* **2022**, *435*, 128997. [[CrossRef](#)]
153. Buss, W.; Graham, M.C.; MacKinnon, G.; Mašek, O. Strategies for producing biochars with minimum PAH contamination. *J. Anal. Appl. Pyrolysis* **2016**, *119*, 24–30. [[CrossRef](#)]
154. Sparrevik, M.; Adam, C.; Martinsen, V.; Jubaedah; Cornelissen, G. Emissions of gases and particles from charcoal/biochar production in rural areas using medium-sized traditional and improved “retort” kilns. *Biomass Bioenergy* **2015**, *72*, 65–73. [[CrossRef](#)]
155. Brouček, J.; Čermák, B. Emission of harmful gases from poultry farms and possibilities of their reduction. *Ekológia* **2015**, *34*, 89–100. [[CrossRef](#)]
156. Giwa, A.; Yusuf, A.; Ajumobi, O.; Dzidzienyo, P. Pyrolysis of date palm waste to biochar using concentrated solar thermal energy: Economic and sustainability implications. *Waste Manag.* **2019**, *93*, 14–22. [[CrossRef](#)]
157. Zeng, K.; Gauthier, D.; Minh, D.P.; Weiss-Hortala, E.; Nzihou, A.; Flamant, G. Characterization of solar fuels obtained from beech wood solar pyrolysis. *Fuel* **2017**, *188*, 285–293. [[CrossRef](#)]
158. Severy, M.A.; Carter, D.J.; Palmer, K.D.; Eggink, A.J.; Chamberlin, C.E.; Jacobson, A.E. Performance and emissions control of commercial-scale biochar production unit. *Appl. Eng. Agric.* **2018**, *34*, 73–84. [[CrossRef](#)]

159. Ahmed, M.B.; Zhou, J.L.; Ngo, H.H.; Guo, W. Insight into biochar properties and its cost analysis. *Biomass Bioenergy* **2016**, *84*, 76–86. [[CrossRef](#)]
160. Alhashimi, H.A.; Aktas, C.B. Life cycle environmental and economic performance of biochar compared with activated carbon: A meta-analysis. *Resour. Conserv. Recycl.* **2017**, *118*, 13–26. [[CrossRef](#)]
161. Tan, R.R. Data challenges in optimizing biochar-based carbon sequestration. *Renew. Sustain. Energy Rev.* **2019**, *104*, 174–177. [[CrossRef](#)]
162. Woolf, D.; Amonette, J.E.; Street-Perrott, F.A.; Lehmann, J.; Joseph, S. Sustainable biochar to mitigate global climate change. *Nat. Commun.* **2010**, *1*, 56. [[CrossRef](#)]
163. McLaren, D. A comparative global assessment of potential negative emissions technologies. *Process Saf. Environ. Prot.* **2012**, *90*, 489–500. [[CrossRef](#)]
164. Hernandez-Soriano, M.C.; Kerré, B.; Goos, P.; Hardy, B.; Dufey, J.; Smolders, E. Long-term effect of biochar on the stabilization of recent carbon: Soils with historical inputs of charcoal. *GCB Bioenergy* **2016**, *8*, 371–381. [[CrossRef](#)]
165. Shakoor, A.; Arif, M.S.; Shahzad, S.M.; Farooq, T.H.; Ashraf, F.; Altaf, M.M.; Ahmed, W.; Tufail, M.A.; Ashraf, M. Does biochar accelerate the mitigation of greenhouse gaseous emissions from agricultural soil?-A global meta-analysis. *Environ. Res.* **2021**, *202*, 111789. [[CrossRef](#)] [[PubMed](#)]
166. Brick, S.; Lyutse, S. *Biochar: Assessing the Promise and Risks to Guide US Policy*; Natural Resources Defense Council: New York, NY, USA, 2010. Available online: <https://www.yumpu.com/en/document/read/37729397/biochar-assessing-the-promise-and-risks-international-biochar-> (accessed on 5 July 2023).
167. Pourhashem, G.; Hung, S.Y.; Medlock, K.B.; Masiello, C.A. Policy support for biochar: Review and recommendations. *GCB Bioenergy* **2019**, *11*, 364–380. [[CrossRef](#)]
168. IBI Standardized Product Definition and Product Testing Guidelines for Biochar. Available online: <https://biochar-international.org/ibi-biochar-standards/> (accessed on 5 July 2023).
169. Guo, M.; He, Z.; Uchimiya, S.M. Introduction to biochar as an agricultural and environmental amendment. *Agric. Environ. Appl. Biochar Adv. Barriers* **2016**, *63*, 1–14.

Disclaimer/Publisher’s Note: The statements, opinions and data contained in all publications are solely those of the individual author(s) and contributor(s) and not of MDPI and/or the editor(s). MDPI and/or the editor(s) disclaim responsibility for any injury to people or property resulting from any ideas, methods, instructions or products referred to in the content.